

## Electroweak Precision Observables: Two-Loop Yukawa Corrections of Supersymmetric Particles

J. HAESTIER<sup>1\*</sup>, S. HEINEMEYER<sup>2†</sup>, D. STÖCKINGER<sup>1‡</sup> AND G. WEIGLEIN<sup>1§</sup>

<sup>1</sup>*IPPP, University of Durham, Durham DH1 3LE, U.K.*

<sup>2</sup>*CERN, TH Division, Dept. of Physics, 1211 Geneva 23, Switzerland*

### Abstract

The dominant electroweak two-loop corrections to the precision observables  $M_W$  and  $\sin^2 \theta_{\text{eff}}$  are calculated in the MSSM. They are obtained by evaluating the two-loop Yukawa contributions of  $\mathcal{O}(\alpha_t^2)$ ,  $\mathcal{O}(\alpha_t \alpha_b)$ ,  $\mathcal{O}(\alpha_b^2)$  to the quantity  $\Delta\rho$ . The result, involving the contributions from Standard Model fermions, sfermions, Higgs bosons and higgsinos, is derived in the gauge-less limit for arbitrary values of the lightest  $\mathcal{CP}$ -even Higgs boson mass. A thorough discussion of the parameter relations enforced by supersymmetry is given, and two different renormalization schemes are applied. Compared to the previously known result for the quark-loop contribution we find a shift of up to +8 MeV in  $M_W$  and  $-4 \times 10^{-5}$  in  $\sin^2 \theta_{\text{eff}}$ . Detailed numerical estimates of the remaining uncertainties of  $M_W$  and  $\sin^2 \theta_{\text{eff}}$  from unknown higher-order contributions are obtained for different values of the supersymmetric mass scale.

---

\*email: J.J.Haestier@durham.ac.uk

†email: Sven.Heinemeyer@cern.ch

‡email: Dominik.Stockinger@durham.ac.uk

§email: Georg.Weiglein@durham.ac.uk

# 1 Introduction

Electroweak precision observables (EWPO) like the masses of the  $W$  and  $Z$  bosons,  $M_{W,Z}$ , or the effective leptonic weak mixing angle,  $\sin^2 \theta_{\text{eff}}$ , are highly sensitive probes of the quantum structure of the electroweak interactions. The Standard Model (SM) and any extension or alternative predicts certain relations between these observables that can be tested against the corresponding experimental values. The experimental resolution is better than the per-mille level [1], and thus the measurements can be sensitive to even two-loop effects. Hence the EWPO are very powerful for discriminating between different models of electroweak interactions and for deriving indirect constraints on unknown parameters such as the masses of the SM Higgs boson or supersymmetric particles, see Ref. [2] for a review. A recent analysis [3] considered the EWPO, combined with the anomalous magnetic moment of the muon and the decay  $b \rightarrow s\gamma$ , in the constrained MSSM with cold dark matter bounds. Already at the current level of experimental and theoretical precisions the sensitivity of the EWPO to the scale of supersymmetry allows to infer interesting information, pointing towards a relatively low scale of supersymmetric particles.

The current experimental accuracies, obtained at LEP, SLC and the Tevatron, for  $M_W$ ,  $M_Z$  and  $\sin^2 \theta_{\text{eff}}$  are  $\delta M_W = 34$  MeV (0.04%),  $\delta M_Z = 2.1$  MeV (0.002%) and  $\delta \sin^2 \theta_{\text{eff}} = 16 \times 10^{-5}$  (0.07%) [1]. At the GigaZ option of a linear  $e^+e^-$  collider, a precision of  $\delta M_W = 7$  MeV [4, 5] and  $\delta \sin^2 \theta_{\text{eff}} = 1.3 \times 10^{-5}$  [5, 6] can be achieved.

The evaluation of the SM theory predictions has reached a high level of sophistication. The one-loop results for the  $M_W$ – $M_Z$  mass relation, parametrized by the quantity  $\Delta r$ , and for  $\sin^2 \theta_{\text{eff}}$  are completely known. For  $\Delta r$  also the full two-loop contributions are known [7, 8], while for  $\sin^2 \theta_{\text{eff}}$  the calculation of all two-loop contributions involving a closed fermion loop has recently been completed [9, 10]. Leading universal corrections to the EWPO in the SM and extensions of it enter via a quantity called  $\Delta\rho$ . It parametrizes the leading universal corrections from vector boson self energies induced by the mass splitting between fields in an isospin doublet [11]. Within the SM various two- and three-loop corrections have been obtained [12–19]. A contribution to  $\Delta\rho$  induces the following shifts in  $M_W$  and  $\sin^2 \theta_{\text{eff}}$  (with  $1 - s_w^2 \equiv c_w^2 = M_W^2/M_Z^2$ ):

$$\Delta M_W \approx \frac{M_W}{2} \frac{c_w^2}{c_w^2 - s_w^2} \Delta\rho, \quad \Delta \sin^2 \theta_{\text{eff}} \approx -\frac{c_w^2 s_w^2}{c_w^2 - s_w^2} \Delta\rho. \quad (1)$$

In the minimal supersymmetric extension of the SM (MSSM) [20], the theoretical evaluation of the EWPO is not as advanced as in the SM. In order to fully exploit the experimental precision for testing the MSSM and deriving constraints on the supersymmetric parameters, it is desirable to reduce the theoretical uncertainty of the MSSM predictions to the same level as the SM uncertainties. So far, the one-loop contributions to  $\Delta r$  and  $\sin^2 \theta_{\text{eff}}$  have been evaluated completely [21, 22]. In the case of non-minimal flavor violation the leading one-loop contributions are known [23]. At the two-loop level, the leading  $\mathcal{O}(\alpha\alpha_s)$  corrections to  $\Delta\rho$  [24] and the gluonic two-loop corrections to  $\Delta r$  [2, 25] are known.

In the present paper we calculate the two-loop MSSM-corrections to the EWPO that enter via  $\Delta\rho$  at  $\mathcal{O}(\alpha_t^2)$ ,  $\mathcal{O}(\alpha_t\alpha_b)$ ,  $\mathcal{O}(\alpha_b^2)$ . These are the leading two-loop contributions involving the top and bottom Yukawa couplings and come from three classes of diagrams with quark/squark loop and additional Higgs or Higgsino exchange (sample diagrams for the three

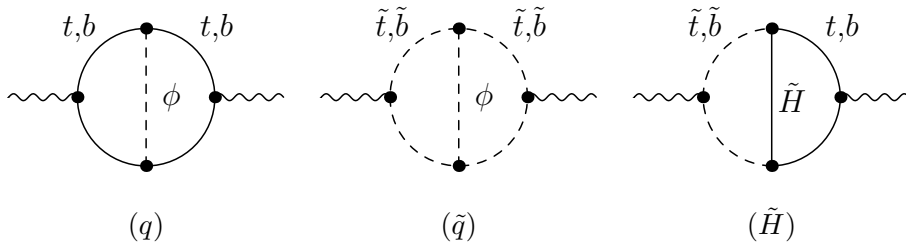


Figure 1: Sample diagrams for the three classes of contributions to  $\Delta\rho$  considered in this paper:  $(q)$  quark loop with Higgs exchange,  $(\tilde{q})$  squark loop with Higgs exchange,  $(\tilde{H})$  quark/squark loop with Higgsino exchange.  $\phi$  denotes Higgs and Goldstone boson exchange.

classes are shown in Fig. 1). These contributions are of particular interest, since they involve corrections proportional to  $m_t^4$  and bottom loop corrections enhanced by  $\tan\beta$ , the ratio of the vacuum expectation values of the two Higgs doublets of the MSSM. Partial results have already been presented in Ref. [26].

As a first step, in Ref. [27] the  $\mathcal{O}(\alpha_t^2)$ ,  $\mathcal{O}(\alpha_t\alpha_b)$ ,  $\mathcal{O}(\alpha_b^2)$  corrections were calculated in the limit where the scalar quarks are heavy, corresponding to taking into account quark/Higgs diagrams (class  $(q)$ ) only. While this class of corrections turned out to be well approximated by the SM contribution (setting the Higgs-boson mass of the SM to the value of the  $\mathcal{CP}$ -even Higgs-boson mass of the MSSM), a potentially larger effect can be expected from diagrams with squarks and higgsinos, classes  $(\tilde{q})$ ,  $(\tilde{H})$  in Fig. 1, which do not possess a SM counterpart. In the related case of similar two-loop corrections to  $(g-2)_\mu$  the squark contributions turned out to be much more important than the quark contributions [28].

For the two-loop Yukawa corrections in the SM it turned out that the dependence on the Higgs-boson mass is numerically important. While the Higgs-boson mass is a free parameter in the SM, the masses of the  $\mathcal{CP}$ -even Higgs bosons of the MSSM are given in terms of the other parameters of the model. In the “gauge-less limit” that has to be applied in order to extract the leading two-loop Yukawa corrections, the mass of the lighter  $\mathcal{CP}$ -even Higgs boson,  $M_h$ , formally has to be put to zero. In Ref. [27] it was observed for the calculation of the diagrams of class  $(q)$  that  $M_h$  can be set to its true value instead of zero in a consistent way. In the present paper we provide a detailed discussion of the gauge-less limit, yielding an explanation of this observation. We will analyze the Higgs-mass dependence also for the other classes of diagrams in Fig. 1.

We analyze the numerical effects of the new corrections for various scenarios in the unconstrained MSSM and for SPS benchmark scenarios [29]. We study two different renormalization schemes and investigate the possible effects of unknown higher-order corrections for  $M_W$  and  $\sin^2\theta_{\text{eff}}$ .

The outline of the paper is as follows. First we review the theoretical status of the EWPO, focusing on the role of  $\Delta\rho$  and the gauge-less limit (Sect. 2), then we describe the structure of the calculation (Sect. 3). In Sect. 4 the renormalization is discussed, taking into account the implications of the gauge-less limit. The numerical analysis is performed in Sect. 5. We conclude with Sect. 6.

## 2 Existing corrections to $\Delta\rho$ in the MSSM

The quantity  $\Delta\rho$ ,

$$\Delta\rho = \frac{\Sigma_Z(0)}{M_Z^2} - \frac{\Sigma_W(0)}{M_W^2}, \quad (2)$$

parametrizes the leading universal corrections to the electroweak precision observables induced by the mass splitting between fields in an isospin doublet [11].  $\Sigma_{Z,W}(0)$  denote the transverse parts of the unrenormalized  $Z$  and  $W$  boson self-energies at zero momentum transfer, respectively. The corresponding shifts in the predictions of  $M_W$  and  $\sin^2\theta_{\text{eff}}$  have been given in eq. (1).

A detailed overview of the existing corrections to the EWPO within the SM and the MSSM can be found in Ref. [2]. Here we briefly review the existing corrections to  $\Delta\rho$  in the MSSM and the corresponding SM contributions. Since  $\Delta\rho$  as defined in eq. (2) is not a physical observable but contains only a part of the quantum corrections to the EWPO, some care has to be taken in its evaluation. Only contributions that form a complete subset of leading corrections to the EWPO can be consistently incorporated into  $\Delta\rho$ . While the fermion loop contributions to  $\Delta\rho$  form a meaningful subset of the full one-loop corrections to the EWPO (see below), a naive evaluation of eq. (2) for the bosonic one-loop contributions of the SM would result in an expression that is neither UV-finite nor gauge-parameter independent (see the discussion in Refs. [2, 30]). A consistent inclusion of the bosonic corrections therefore makes it necessary to go beyond the  $\Delta\rho$  approximation. We will introduce the so-called ‘‘gauge-less limit’’ in Sect. 2.2 and show that at  $\mathcal{O}(\alpha_t^2)$ ,  $\mathcal{O}(\alpha_t\alpha_b)$ ,  $\mathcal{O}(\alpha_b^2)$  the contributions to  $\Delta\rho$  coincide with the complete contributions to the EWPO.

### 2.1 One-loop and higher-order QCD corrections to $\Delta\rho$

The dominant one-loop contribution to  $\Delta\rho$  within the SM arises from the top/bottom doublet [11]. It is given by

$$\Delta\rho_{1\text{-loop}}^{\text{SM}} = \frac{3G_\mu}{8\sqrt{2}\pi^2} F_0(m_t^2, m_b^2), \quad (3)$$

where

$$F_0(x, y) = x + y - \frac{2xy}{x-y} \log \frac{x}{y}. \quad (4)$$

$F_0$  has the properties  $F_0(m_1^2, m_2^2) = F_0(m_2^2, m_1^2)$ ,  $F_0(m^2, m^2) = 0$ ,  $F_0(m^2, 0) = m^2$ . One therefore obtains  $F_0(m_t^2, m_b^2) \approx m_t^2$ , giving rise to the well-known quadratic dependence of the one-loop corrections to the EWPO on the top-quark mass.

Within the MSSM the dominant correction from supersymmetric particles at the one-loop level arises from the scalar top and bottom contribution to eq. (2). For  $m_b \neq 0$  it is given by

$$\begin{aligned} \Delta\rho_{1\text{-loop}}^{\text{SUSY}} = \frac{3G_\mu}{8\sqrt{2}\pi^2} \Big[ & -\sin^2\theta_{\bar{t}} \cos^2\theta_{\bar{t}} F_0(m_{\bar{t}_1}^2, m_{\bar{t}_2}^2) - \sin^2\theta_{\bar{b}} \cos^2\theta_{\bar{b}} F_0(m_{\bar{b}_1}^2, m_{\bar{b}_2}^2) \\ & + \cos^2\theta_{\bar{t}} \cos^2\theta_{\bar{b}} F_0(m_{\bar{t}_1}^2, m_{\bar{b}_1}^2) + \cos^2\theta_{\bar{t}} \sin^2\theta_{\bar{b}} F_0(m_{\bar{t}_1}^2, m_{\bar{b}_2}^2) \\ & + \sin^2\theta_{\bar{t}} \cos^2\theta_{\bar{b}} F_0(m_{\bar{t}_2}^2, m_{\bar{b}_1}^2) + \sin^2\theta_{\bar{t}} \sin^2\theta_{\bar{b}} F_0(m_{\bar{t}_2}^2, m_{\bar{b}_2}^2) \Big]. \quad (5) \end{aligned}$$

Here  $m_{\tilde{t}_i}, m_{\tilde{b}_i}$  ( $i = 1, 2$ ) denote the stop and sbottom masses, whereas  $\theta_{\tilde{t}}, \theta_{\tilde{b}}$  are the mixing angles in the stop and in the sbottom sector, see also Sect. 3.1.1.

The dominant two-loop correction within the SM of  $\mathcal{O}(\alpha\alpha_s)$  is given by [12]

$$\Delta\rho_{2\text{-loop}}^{\text{SM},\alpha\alpha_s} = -\Delta\rho_{1\text{-loop}}^{\text{SM}} \frac{2}{3} \frac{\alpha_s}{\pi} (1 + \pi^2/3). \quad (6)$$

It screens the one-loop result by approximately 10%.

The corresponding corrections of  $\mathcal{O}(\alpha\alpha_s)$  in the MSSM have been evaluated in Ref. [24]. Contrary to the SM case, these corrections can enter with the same sign as the one-loop result, therefore enhancing the sensitivity to the squark effects.

## 2.2 Electroweak two-loop corrections to $\Delta\rho$ : the gauge-less limit

The Yukawa contributions of  $\mathcal{O}(\alpha_f^2)$  form a set of leading two-loop contributions entering the EWPO only via  $\Delta\rho$ , where  $\alpha_f \equiv y_f^2/(4\pi)$ , and  $y_f$  is the Yukawa coupling of fermion  $f$ . For the top and bottom quarks the Yukawa couplings read

$$y_t = \frac{\sqrt{2} m_t}{v \sin \beta}, \quad y_b = \frac{\sqrt{2} m_b}{v \cos \beta}, \quad (7)$$

where  $v \equiv \sqrt{v_1^2 + v_2^2}$ . In the SM another subset of leading electroweak two-loop corrections to  $\Delta\rho$  is given by the corrections for large Higgs-boson masses of  $\mathcal{O}(G_\mu^2 M_H^2 M_W^2)$  [16]. We will focus on the Yukawa corrections in the following.

In order to evaluate the leading Yukawa contributions of  $\mathcal{O}(\alpha_f^2)$  the gauge-less limit has to be applied. It consists of neglecting the electroweak gauge couplings  $g_{1,2} \rightarrow 0$  and thus also  $M_W^2 = g_2^2 v^2/2 \rightarrow 0$  and  $M_Z^2 = (g_1^2 + g_2^2)v^2/2 \rightarrow 0$ , while keeping the ratio  $c_w = M_W/M_Z$  and the vacuum expectation value  $v$  fixed. Accordingly,  $\Sigma_{Z,W}$  in eq. (2) need to be evaluated at  $\mathcal{O}(g_{1,2}^0)$  in order to obtain a finite contribution of  $\mathcal{O}(g_{1,2}^0)$  to  $\Delta\rho$  in the gauge-less limit. In this limit only diagrams with fermions and scalars contribute to  $\Delta\rho$ , while no gauge bosons appear in the loop diagrams.

At the one-loop level the only non-vanishing contributions to  $\Delta\rho$  in the gauge-less limit of the MSSM are the fermion-loop and sfermion-loop contributions as given in eqs. (3), (5). While the Higgs sector of a general two-Higgs-doublet model yields a contribution to  $\Delta\rho$  in the gauge-less limit, the contribution vanishes once the symmetry relations of the MSSM are imposed (see the discussion in Sect. 4.1 below).

At the two-loop level the gauge-less limit results in the desired Yukawa contributions of  $\mathcal{O}(\alpha_f^2)$ . For the quarks and squarks of the third generation this yields in particular terms of  $\mathcal{O}(m_t^4/v^4)$  and  $\mathcal{O}(m_b^4 \tan^2 \beta/v^4)$ . It is easy to see that no other contribution to  $M_W$  and  $\sin^2 \theta_{\text{eff}}$  besides the gauge-less limit of  $\Delta\rho$  yields terms of this order.

In the SM the two-loop result for  $\Delta\rho$  in the gauge-less limit was first obtained for the special case  $M_{H^{\text{SM}}} = 0$  [14],

$$\Delta\rho_{2\text{-loop}|M_H=0}^{\text{SM},\alpha_t^2} = 3 \frac{G_\mu^2}{128\pi^4} m_t^4 (19 - 2\pi^2). \quad (8)$$

This result was then extended to the case of arbitrary values of  $M_{H^{\text{SM}}}$  [15]. The corresponding result is given by

$$\begin{aligned}
\Delta\rho_{2\text{-loop}}^{\text{SM},\alpha_t^2}(M_{H^{\text{SM}}}) &= 3\frac{G_\mu^2}{128\pi^4}m_t^4\left\{-3\frac{x^2(10-6x^2+x^4)}{x^2-4}w\log^2\left(\frac{1-w}{2}\right)\right. \\
&\quad +\frac{x^2(x^2-4)}{2}w\log\left(\frac{1-w}{1+w}\right) \\
&\quad -\left(6+6x^2-\frac{x^4}{2}\right)\log(x^2)+3\frac{x^2(10-6x^2+x^4)}{2(x^2-4)}w\log^2(x^2) \\
&\quad +25-4x^2+\pi^2\frac{+8-6x^2+x^4-10wx^4+6wx^6-wx^8}{2x^2(x^2-4)} \\
&\quad +6wx^2\frac{10-6x^2+x^4}{x^2-4}\text{Li}_2\left(\frac{1-w}{2}\right) \\
&\quad \left.-\frac{3(x^2-1)^2(x^2-2)}{x^2}\text{Li}_2(1-x^2)\right\}, \tag{9}
\end{aligned}$$

where  $x = M_{H^{\text{SM}}}/m_t$ , and  $w = \sqrt{1-4/x^2}$ . The effect of going beyond the approximation  $M_{H^{\text{SM}}} = 0$  turned out to be numerically very significant. While the numerical value of the result in eq. (8) is rather small due to the accidental cancellation of the two terms in the last factor of eq. (8), the result is about an order of magnitude larger for values of  $M_{H^{\text{SM}}}$  in the experimentally preferred region. As a consequence, the result for the  $\mathcal{O}(\alpha_t^2)$  corrections to  $\Delta\rho$  with arbitrary Higgs-boson mass as given in eq. (9) provides a much better approximation of the full electroweak two-loop corrections to the EWPO [7–10] than the limiting case where  $M_{H^{\text{SM}}} = 0$ , eq. (8). As an example, for  $M_{H^{\text{SM}}} = 120$  GeV the resulting shifts in  $M_W$  and  $\sin^2\theta_{\text{eff}}$  are  $-10$  MeV and  $+5 \times 10^{-5}$ , respectively.

Within the MSSM also the contributions involving the bottom Yukawa coupling can be relevant at large  $\tan\beta$ . The corresponding contributions of  $\mathcal{O}(\alpha_t^2)$ ,  $\mathcal{O}(\alpha_t\alpha_b)$ , and  $\mathcal{O}(\alpha_b^2)$  to  $\Delta\rho$  have been obtained in Ref. [27] in the limit of heavy scalar quarks. In this limit only the top and bottom quarks and the Higgs bosons (and Goldstone bosons) of the MSSM appear in the loops. The results turned out to be numerically relevant, leading to shifts in  $M_W$  and  $\sin^2\theta_{\text{eff}}$  of up to 12 MeV and  $6 \times 10^{-5}$ , respectively. Since in the gauge-less limit the couplings of the light  $\mathcal{CP}$ -even Higgs boson of the MSSM to fermions become SM-like, the  $\mathcal{O}(\alpha_t^2)$  correction in the MSSM can be well approximated by the corresponding correction in the SM, as given in eq. (9). Potentially larger effects compared to the SM case can be expected from the contribution of supersymmetric particles (with not too heavy masses), since these corrections do not have a SM counterpart.

### 3 The $\mathcal{O}(\alpha_t^2)$ , $\mathcal{O}(\alpha_t\alpha_b)$ , $\mathcal{O}(\alpha_b^2)$ contributions to $\Delta\rho$

The purpose of the present paper is to perform a complete calculation of the  $\mathcal{O}(\alpha_t^2)$ ,  $\mathcal{O}(\alpha_t\alpha_b)$ , and  $\mathcal{O}(\alpha_b^2)$  contributions to  $\Delta\rho$  in the MSSM, including the contributions of supersymmetric particles. This means that all diagrams have to be evaluated (applying the gauge-less limit) that contain top and bottom quarks, their scalar superpartners stop and sbottom, and Higgs bosons or higgsinos.

The contributions to  $\Delta\rho$  at  $\mathcal{O}(\alpha_t^2)$ ,  $\mathcal{O}(\alpha_t\alpha_b)$ ,  $\mathcal{O}(\alpha_b^2)$  can be grouped into three classes (see Fig. 1):

- ( $q$ ) diagrams involving  $t/b$  quarks and Higgs bosons (see also Ref. [27]),
- ( $\tilde{q}$ ) diagrams with  $\tilde{t}/\tilde{b}$  squarks and Higgs bosons (see Fig. 2 for generic diagrams),
- ( $\tilde{H}$ ) diagrams with higgsinos (containing also quarks and squarks) (see Fig. 3 for generic diagrams).

The generic diagrams shown in Figs. 2, 3 have to be evaluated for the  $Z$  boson and the  $W$  boson self-energy.

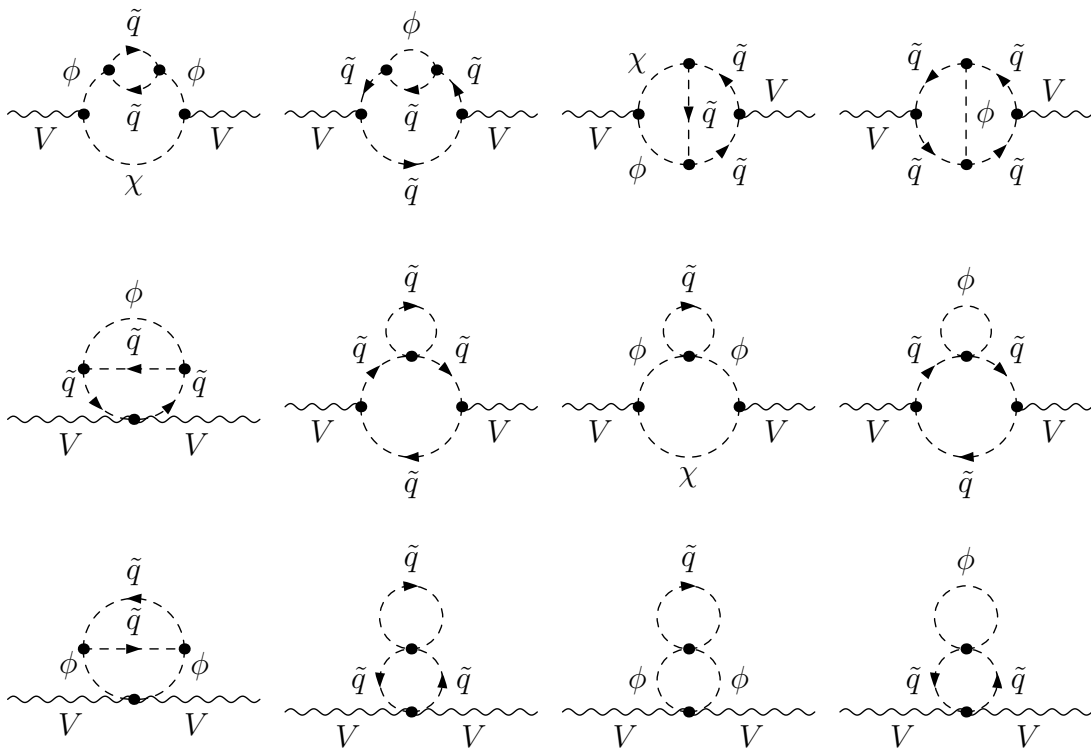


Figure 2: Generic Feynman diagrams of class ( $\tilde{q}$ ).  $V$  denotes either  $W$  or  $Z$ ,  $\tilde{q}$  is either a  $\tilde{t}$  or a  $\tilde{b}$ , and  $\phi, \chi$  denote Higgs and Goldstone bosons.

In the following sections we describe the necessary ingredients for the evaluation of these contributions, starting with the relevant sectors of the MSSM and then turning to the technical evaluation of the two-loop diagrams and the counterterms.

### 3.1 The relevant MSSM sectors

Here we specify the MSSM contributions that are relevant for the  $\mathcal{O}(\alpha_t^2)$ ,  $\mathcal{O}(\alpha_t\alpha_b)$ ,  $\mathcal{O}(\alpha_b^2)$  corrections. As explained above, the calculation involves the gauge-less limit where  $M_W, M_Z \rightarrow$

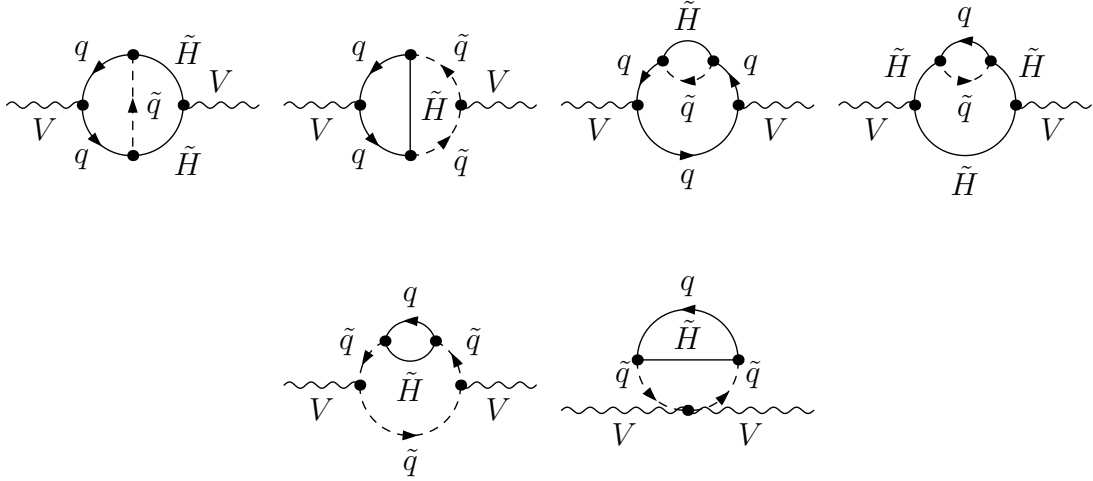


Figure 3: Generic Feynman diagrams of class  $(\tilde{H})$ .  $V$  denotes either  $W$  or  $Z$ ,  $\tilde{q}$  is either a  $\tilde{t}$  or a  $\tilde{b}$ , while  $q$  is a  $t$  or a  $b$ , and  $\tilde{H}$  denotes a higgsino (neutral or charged).

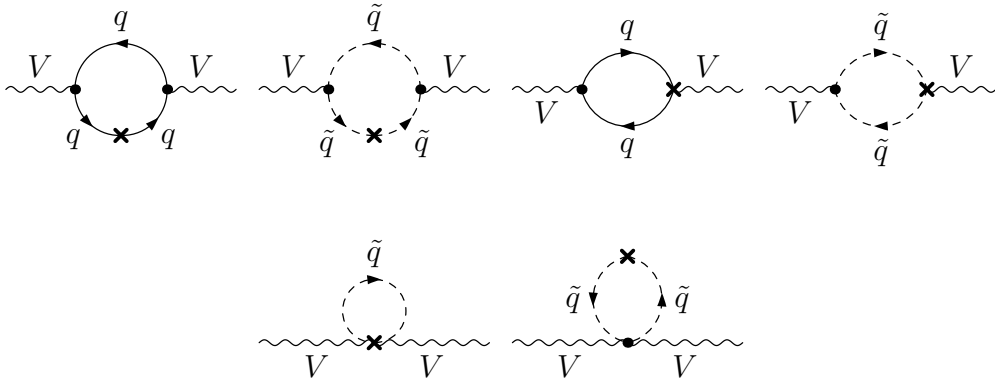


Figure 4: Generic Feynman diagrams for the vector boson self-energies with counterterm insertion.  $V$  denotes either  $W$  or  $Z$ ,  $\tilde{q}$  is either a  $\tilde{t}$  or a  $\tilde{b}$ , while  $q$  is a  $t$  or a  $b$

0 (keeping  $c_w = M_W/M_Z$  fixed). Accordingly, we discuss the implications of the gauge-less limit for the different sectors of the MSSM.



### 3.1.1 The scalar top and bottom sector

We start with the stop and sbottom sector. In order to fix the notation, we explicitly list their mass matrices in the basis of the interaction eigenstates  $\tilde{t}_L, \tilde{t}_R$  and  $\tilde{b}_L, \tilde{b}_R$ :

$$\mathcal{M}_t^2 = \begin{pmatrix} M_{\tilde{t}_L}^2 + m_t^2 + \cos 2\beta \left(\frac{1}{2} - \frac{2}{3}s_w^2\right)M_Z^2 & m_t X_t \\ m_t X_t & M_{\tilde{t}_R}^2 + m_t^2 + \frac{2}{3} \cos 2\beta s_w^2 M_Z^2 \end{pmatrix}, \quad (10)$$

$$\mathcal{M}_b^2 = \begin{pmatrix} M_{\tilde{b}_L}^2 + m_b^2 + \cos 2\beta \left(-\frac{1}{2} + \frac{1}{3}s_w^2\right)M_Z^2 & m_b X_b \\ m_b X_b & M_{\tilde{b}_R}^2 + m_b^2 - \frac{1}{3} \cos 2\beta s_w^2 M_Z^2 \end{pmatrix} \quad (11)$$

where

$$m_t X_t \equiv m_t (A_t - \mu \cot \beta), \quad m_b X_b \equiv m_b (A_b - \mu \tan \beta). \quad (12)$$

Here  $A_t$  denotes the trilinear Higgs–stop coupling,  $A_b$  denotes the Higgs–sbottom coupling, and  $\mu$  is the higgsino mass parameter.

In order to obtain the mass eigenvalues the mass matrix has to be diagonalized. This is done with the help of the unitary matrix  $U^{\tilde{q}}$ ,

$$U^{\tilde{q}} \mathcal{M}_q^2 U^{\tilde{q}\dagger} = \text{diag}(m_{\tilde{q}_1}^2, m_{\tilde{q}_2}^2), \quad q = t, b, \quad (13)$$

which we will choose real since we consider the MSSM without  $\mathcal{CP}$ -violation.

Furthermore, SU(2) gauge invariance requires the relation

$$M_{\tilde{t}_L}^2 = M_{\tilde{b}_L}^2 \quad (14)$$

between the soft supersymmetry-breaking parameters in the left-handed components of the squark doublet. Consequently, there are only five independent parameters in the  $\tilde{t}/\tilde{b}$  sector. The masses and mixing angles are connected via the relation

$$\sum_{i=1,2} |U_{i1}^{\tilde{b}}|^2 m_{\tilde{b}_i}^2 = \sum_{i=1,2} |U_{i1}^{\tilde{t}}|^2 m_{\tilde{t}_i}^2 + m_b^2 - m_t^2 - M_Z^2 c_w^2 \cos 2\beta. \quad (15)$$

In the gauge-less limit the terms proportional to  $M_Z^2$  in the diagonal entries of the mass matrices and in eq. (15) vanish.

Except where stated otherwise, we will assume universality of all three soft supersymmetry-breaking parameters in the diagonal entries of the stop/sbottom mass matrices,

$$M_{\text{SUSY}} \equiv M_{\tilde{t}_L} = M_{\tilde{t}_R} = M_{\tilde{b}_R}. \quad (16)$$

The common squark mass scale is denoted as  $M_{\text{SUSY}}$ .

### 3.1.2 The Higgs sector

Contrary to the SM, in the MSSM two Higgs doublets are required [31]. At the tree-level, the Higgs sector can be described with the help of two independent parameters (besides  $g_1$  and  $g_2$ ): the ratio of the two vacuum expectation values,  $\tan \beta = v_2/v_1$ , and  $M_A$ , the mass of the  $\mathcal{CP}$ -odd  $A$  boson. The diagonalization of the bilinear part of the Higgs potential, i.e.

the Higgs mass matrices, is performed via orthogonal transformations with the angle  $\alpha$  for the  $\mathcal{CP}$ -even part and with the angle  $\beta$  for the  $\mathcal{CP}$ -odd and the charged part. The mixing angle  $\alpha$  is determined through

$$\tan 2\alpha = \tan 2\beta \frac{M_A^2 + M_Z^2}{M_A^2 - M_Z^2}; \quad -\frac{\pi}{2} < \alpha < 0. \quad (17)$$

One gets the following Higgs spectrum:

$$\begin{aligned} 2 \text{ neutral bosons, } \mathcal{CP} = +1 & : h, H \\ 1 \text{ neutral boson, } \mathcal{CP} = -1 & : A \\ 2 \text{ charged bosons} & : H^+, H^- \\ 3 \text{ unphysical Goldstone bosons} & : G^0, G^+, G^-. \end{aligned} \quad (18)$$

At the tree level, the Higgs boson masses expressed through  $M_Z$ ,  $M_W$  and  $M_A$  are given by

$$M_h^2 = \frac{1}{2} \left[ M_A^2 + M_Z^2 - \sqrt{(M_A^2 + M_Z^2)^2 - 4M_A^2 M_Z^2 \cos^2 2\beta} \right], \quad (19)$$

$$M_H^2 = \frac{1}{2} \left[ M_A^2 + M_Z^2 + \sqrt{(M_A^2 + M_Z^2)^2 - 4M_A^2 M_Z^2 \cos^2 2\beta} \right], \quad (20)$$

$$M_{H^\pm}^2 = M_A^2 + M_W^2. \quad (21)$$

We use the Feynman gauge, which implies the mass parameters  $M_G^2 = M_Z^2$ ,  $M_{G^\pm}^2 = M_W^2$  for the unphysical scalars  $G^0$  and  $G^\pm$ .

In the gauge-less limit the Higgs sector parameters satisfy the following relations:

$$M_{H^\pm}^2 = M_H^2 = M_A^2, \quad (22a)$$

$$\sin \alpha = -\cos \beta, \quad \cos \alpha = \sin \beta, \quad (22b)$$

$$M_G^2 = M_{G^\pm}^2 = 0. \quad (22c)$$

In the gauge-less limit furthermore the mass of the lightest  $\mathcal{CP}$ -even Higgs boson vanishes at tree level,

$$M_h = 0. \quad (23)$$

Because of the accidental cancellation in the SM result for  $M_{H^{\text{SM}}} = 0$ , see eq. (8), it is desirable to retain the dependence on  $M_h$  as much as possible in the MSSM result. In this way the numerical impact of the  $M_h$ -dependence can be studied, which within the MSSM is formally a higher-order effect. This is particularly interesting in view of the fact that higher-order corrections to the masses and mixing angles in the MSSM Higgs sector are sizable, see e.g. Ref. [32] for recent reviews.

We will therefore discuss the implementation of the gauge-less limit in some detail. In particular, we will investigate in how far a consistent result for  $\Delta\rho$  can be obtained without imposing eq. (23). We will also briefly discuss the case where eq. (22b) is relaxed, see Sect. 4 below. For higher-order corrections in the Higgs sector we use the results as implemented into the code *FeynHiggs* [33–36].

### 3.1.3 Higgsinos

In the gauge-less limit the contributions from the chargino and neutralino sector reduce to those of the higgsinos.

The diagonalization matrices for the chargino and neutralino sectors in this limit are given by (see Ref. [2] for our notation)

$$\mathbf{U} = \mathbf{V} = \begin{pmatrix} 0 & 0 \\ 0 & 1 \end{pmatrix}, \quad \mathbf{N} = \frac{1}{\sqrt{2}} \begin{pmatrix} 0 & 0 & 0 & 0 \\ 0 & 0 & 0 & 0 \\ 0 & 0 & 1 & -1 \\ 0 & 0 & 1 & 1 \end{pmatrix}, \quad (24)$$

and the corresponding elements of the diagonalized mass matrices are

$$m_{\tilde{\chi}_i^\pm} = (0, +\mu), \quad m_{\tilde{\chi}_i^0} = (0, 0, +\mu, -\mu). \quad (25)$$

All entries corresponding to gauginos are zero since the gaugino couplings vanish in the gauge-less limit. Note that the negative sign in  $m_{\tilde{\chi}_4^0}$  has to be taken into account; the physical masses of the charged and neutral higgsinos are all equal to  $+\mu$  in the gauge-less limit.

## 3.2 Evaluation of the Feynman diagrams

The amplitudes of all Feynman diagrams shown in Figs. 2,3,4 have been created with the program *FeynArts3* [37], making use of the MSSM model file [38]. Dirac algebra and traces have been evaluated using the program *TwoCalc* [39], and the reduction to scalar integrals has been performed in two ways using either the package *TYReduce* [40] or the routines built into *TwoCalc*, based on the reduction method of Ref. [39]. As a result we obtained the analytical expression for  $\Delta\rho$  depending on the one-loop functions  $A_0$  and  $B_0$  [41] and on the two-loop function  $T_{134}$  [39, 42]. For the further evaluation the analytical expressions for  $A_0$ ,  $B_0$  and  $T_{134}$  have been inserted.

In addition to the two-loop diagrams, one-loop counterterms corresponding to the renormalization of divergent one-loop subdiagrams have to be taken into account. The whole calculation can be performed both in dimensional regularization [43] as well as in dimensional reduction [44]. Since no gauge bosons appear in the loops, both regularization schemes preserve gauge invariance and supersymmetry for the present calculation. Therefore the necessary counterterms correspond to multiplicative renormalization of the parameters in the MSSM Lagrangian.

## 3.3 Counterterms

The renormalization constants that are relevant in the gauge-less limit are

$$\begin{aligned} \delta m_t, \delta m_b, \delta m_{\tilde{t}_1}^2, \delta m_{\tilde{t}_2}^2, \delta\theta_{\tilde{t}}, \delta m_{\tilde{b}_1}^2, \delta m_{\tilde{b}_2}^2, \delta\theta_{\tilde{b}}, \\ \delta M_A^2, \delta \tan \beta, \delta t_{h,H}, \delta\mu, \end{aligned} \quad (26)$$

corresponding to the renormalization of the fermion masses, the parameters of the  $\tilde{t}/\tilde{b}$  sector, the Higgs sector parameters and tadpoles, and the  $\mu$ -parameter. It is not necessary to introduce wave function renormalization constants for the fermions and scalar fields since they drop out in the sum over all diagrams.

There are two possible ways to obtain the counterterm contributions:

1. Generate and evaluate one-loop diagrams with insertions of counterterm vertices, as depicted generically in Fig. 4. In order to generate these diagrams, the required counterterm Feynman rules had to be added to the *FeynArts* MSSM model file. In the explicit evaluation of the counterterm diagrams it turned out that the renormalization constants  $\delta M_A^2$ ,  $\delta \tan \beta$ ,  $\delta t_{h,H}$ ,  $\delta \mu$ , corresponding to the Higgs/higgsino sector, drop out. Only the quark and squark mass and mixing renormalization constants contribute.
2. The renormalization transformation  $\lambda_i \rightarrow \lambda_i + \delta \lambda_i$  for each parameter  $\lambda_i$  appearing in eq. (26) is performed directly in the one-loop result  $\Delta \rho_{1\text{-loop}}^{\text{SM+SUSY}}(\lambda_i)$ . The counterterm contribution for the two-loop calculation is then obtained by expanding  $\Delta \rho_{1\text{-loop}}^{\text{SM+SUSY}}(\lambda_i + \delta \lambda_i)$  to first order in the  $\delta \lambda_i$ , where the contributions to  $\Delta \rho_{1\text{-loop}}^{\text{SM+SUSY}}$  have been given in eqs. (3), (5). In this setup it is obvious that the renormalization constants  $\delta M_A^2$ ,  $\delta \tan \beta$ ,  $\delta t_{h,H}$ ,  $\delta \mu$  do not contribute, since the one-loop result in the gauge-less limit consists only of the quark and squark loop contributions and therefore does not depend on the Higgs-sector parameters. Accordingly, the counterterm contributions for the two-loop calculation,  $\Delta \rho_{\text{ct}}$ , can be written as

$$\Delta \rho_{\text{ct}} = \sum_{f=t,b} \left( \delta m_f \partial_{m_f} + \sum_{i=1,2} \delta m_{\tilde{f}_i}^2 \partial_{m_{\tilde{f}_i}^2} + \sum_{i,j=1,2} \delta U_{ij}^{\tilde{f}} \partial_{U_{ij}^{\tilde{f}}} \right) \Delta \rho_{1\text{-loop}}^{\text{SM+SUSY}}. \quad (27)$$

In order to have a non-trivial check of the counterterm contributions, we implemented them using both approaches and found agreement in the final result.

Due to supersymmetry and SU(2) gauge invariance, see eq. (14), there are only five independent parameters in the  $\tilde{t}/\tilde{b}$  sector, leading to eq. (15). As a consequence, not all the parameters appearing in eq. (15) can be renormalized independently. Choosing  $m_{\tilde{b}_1}^2$  as the dependent parameter, its counterterm  $\delta m_{\tilde{b}_1}^2$  can be expressed in terms of the other counterterms. In the gauge-less limit the relation reads

$$\begin{aligned} \delta m_{\tilde{b}_1}^2 = \frac{1}{|U_{11}^{\tilde{b}}|^2} & \left( \sum_{i=1,2} |U_{i1}^{\tilde{t}}|^2 \delta m_{\tilde{t}_i}^2 - |U_{21}^{\tilde{b}}|^2 \delta m_{\tilde{b}_2}^2 + 2 U_{11}^{\tilde{t}} U_{21}^{\tilde{t}} (m_{\tilde{t}_1}^2 - m_{\tilde{t}_2}^2) \delta u_{12}^{\tilde{t}} \right. \\ & \left. - 2 U_{11}^{\tilde{b}} U_{21}^{\tilde{b}} (m_{\tilde{b}_1}^2 - m_{\tilde{b}_2}^2) \delta u_{12}^{\tilde{b}} - 2 m_t \delta m_t + 2 m_b \delta m_b \right), \end{aligned} \quad (28)$$

where the renormalization transformation of the mixing matrix is defined as

$$U_{ij}^{\tilde{q}} \rightarrow U_{ij}^{\tilde{q}} + \delta U_{ij}^{\tilde{q}}, \quad \delta U_{ij}^{\tilde{q}} = \delta u_{ik}^{\tilde{q}} U_{kj}^{\tilde{q}}, \quad \delta u_{ij}^{\tilde{q}} = -\delta u_{ji}^{\tilde{q}}. \quad (29)$$

In order to define the renormalization constants one has to choose a renormalization scheme. For the SM fermion masses  $m_{t,b}$  we always choose the on-shell scheme. This yields for the top mass counterterm

$$\delta m_t = \frac{1}{2} m_t \left[ \text{Re} \Sigma_{t_L}(m_t^2) + \text{Re} \Sigma_{t_R}(m_t^2) + 2 \text{Re} \Sigma_{t_S}(m_t^2) \right], \quad (30)$$

with the scalar coefficients of the unrenormalized top-quark self-energy,  $\Sigma_t(p)$ , in the Lorentz decomposition

$$\Sigma_t(p) = \not{p}\omega_{-\Sigma_{t_L}}(p^2) + \not{p}\omega_{+\Sigma_{t_R}}(p^2) + m_t\Sigma_{t_S}(p^2), \quad (31)$$

and analogously for the bottom mass counterterm (in order to take higher-order QCD corrections into account, we use an effective bottom quark mass value of  $m_b = 3$  GeV). For the five independent  $\tilde{t}/\tilde{b}$  sector parameters we choose either the on-shell [45, 46] or the  $\overline{\text{DR}}$  scheme. The precise definitions will be given in the following section.

## 4 Renormalization prescriptions and result for $\Delta\rho$

As explained above, the strict implementation of the gauge-less limit in the evaluation of the  $\mathcal{O}(\alpha_t^2)$ ,  $\mathcal{O}(\alpha_t\alpha_b)$ ,  $\mathcal{O}(\alpha_b^2)$  contributions to  $\Delta\rho$  would imply that the mass of the lightest  $\mathcal{CP}$ -even Higgs boson has to be set to zero, see eq. (23). In the SM case, where  $M_{H^{\text{SM}}}$  is a free parameter, it turned out that the two-loop Yukawa contribution to  $\Delta\rho$  yields a much better approximation of the full electroweak two-loop corrections to the EWPO for (realistic) non-zero values of  $M_{H^{\text{SM}}}$  than in the limit  $M_{H^{\text{SM}}} = 0$ . It is therefore of interest to investigate the impact of non-zero values of  $M_h$  also for the MSSM, where  $M_h$  is a dependent quantity that is determined by the other supersymmetric parameters.

It has been observed already in Ref. [27] that the pure fermion contributions of class ( $q$ ) (see Fig. 1) may consistently be obtained even if eq. (23) is not employed. In this section we discuss this issue in detail and explain the physical origin of this behavior. Based on this result we show how the calculation of all three classes of contributions to  $\Delta\rho$ , i.e. ( $q$ ), ( $\tilde{q}$ ), and ( $\tilde{H}$ ), can be organized in such a way that  $M_h$  can be set to its true MSSM value essentially everywhere. We will use the resulting expression in order to study the numerical effect of non-zero  $M_h$  values for the new corrections calculated in this paper, namely the squark contribution ( $\tilde{q}$ ) and the higgsino contribution ( $\tilde{H}$ ).

### 4.1 Higgs sector

In order to discuss the implementation of the gauge-less limit it is useful to compare the MSSM case with the one of a general two-Higgs-doublet model (2HDM). In the following “2HDM” is to be understood as a two-Higgs-doublet model including squarks and higgsinos, but without any supersymmetric relations imposed on them. The MSSM can be regarded as a special case of a 2HDM, with supersymmetric relations for couplings and masses. In the 2HDM without these coupling relations,  $\Delta\rho$  is also well-defined and can be calculated at  $\mathcal{O}(\alpha_t^2)$ ,  $\mathcal{O}(\alpha_t\alpha_b)$ ,  $\mathcal{O}(\alpha_b^2)$  in the gauge-less limit. The corresponding two-loop diagrams are identical to the diagrams of the classes ( $q$ ), ( $\tilde{q}$ ), ( $\tilde{H}$ ) in the MSSM. However, in contrast to the MSSM, the Higgs-boson masses in the 2HDM are independent parameters and do not have to obey eqs. (22), (23) in the gauge-less limit.

The essential difference between the MSSM and the 2HDM case concerns the renormalization and counterterm contributions. Restricting ourselves in a first step to class ( $q$ ), these contributions can be decomposed in the MSSM and the 2HDM as

$$\Delta\rho_{\text{MSSM}}^{(q)} = \Delta\rho_{2\text{-loop}}^{(q)} + \Delta\rho_{tb\text{-ct}}^{(q)} \quad (32)$$

$$\Delta\rho_{2\text{HDM}}^{(q)} = \Delta\rho_{2\text{-loop}}^{(q)} + \Delta\rho_{tb\text{-ct}}^{(q)} + \Delta\rho_{H\text{-ct}}^{(q)}, \quad (33)$$

respectively. Here the two-loop contribution  $\Delta\rho_{2\text{-loop}}^{(q)}$  and the counterterm contributions from the  $t/b$  doublet  $\Delta\rho_{tb\text{-ct}}^{(q)}$  are identical in the two models, while the Higgs sector counterterm contribution  $\Delta\rho_{H\text{-ct}}^{(q)}$  appears only in the 2HDM result.

As mentioned above, in the MSSM there are no one-loop contributions from the Higgs sector and correspondingly no Higgs sector counterterm contributions at  $\mathcal{O}(\alpha_t^2)$ ,  $\mathcal{O}(\alpha_t\alpha_b)$ ,  $\mathcal{O}(\alpha_b^2)$ . In the 2HDM, the Higgs sector one-loop contribution to  $\Delta\rho$  reads

$$\begin{aligned} \Delta\rho_{1\text{-loop}}^{2\text{HDM}} = \frac{g^2}{128\pi^2 M_W^2} & \left[ F_0(M_{H^\pm}^2, M_A^2) \right. \\ & + \sin^2(\beta - \alpha) (F_0(M_{H^\pm}^2, M_H^2) - F_0(M_A^2, M_H^2)) \\ & \left. + \cos^2(\beta - \alpha) (F_0(M_{H^\pm}^2, M_h^2) - F_0(M_A^2, M_h^2)) \right] \quad (34) \end{aligned}$$

in the gauge-less limit. Note that this contribution indeed vanishes if the MSSM gauge-less limit relations (22) hold. The counterterm contribution from the Higgs sector at the two-loop level can be obtained from this expression as

$$\Delta\rho_{H\text{-ct}}^{(q)} \equiv \left( \sum_{\phi=h,H,A^0,H^\pm} \delta M_\phi^2 \partial_{M_\phi^2} + \delta \tan \beta \partial_{\tan \beta} + \delta \sin \alpha \partial_{\sin \alpha} \right) \Delta\rho_{1\text{-loop}}^{2\text{HDM}}. \quad (35)$$

Since  $F_0(x, y)$  and  $\partial_x F_0(x, y)$  vanish in the limit  $x = y$ , we find that  $\Delta\rho_{H\text{-ct}}^{(q)}$  vanishes if

$$M_H = M_{H^\pm} = M_A, \quad \cos(\beta - \alpha) = 0, \quad M_h = \text{arbitrary} \quad (36)$$

or

$$M_{H^\pm} = M_A, \quad \delta M_{H^\pm}^2 = \delta M_A^2, \quad M_h, M_H, \alpha = \text{arbitrary}. \quad (37)$$

The relations in eq. (36) are the same as the constraints imposed by the gauge-less limit in the MSSM except for the fact that  $M_h = 0$  is not necessary. The observation made in Ref. [27] that the class  $(q)$  contributions to  $\Delta\rho$  can be evaluated in the MSSM in a meaningful way for non-zero values of  $M_h$  can be understood from eq. (36). For class  $(q)$  the two-loop diagrams and the fermion sector counterterms are identical in the MSSM and the 2HDM. If the relations in eq. (36) hold,  $\Delta\rho_{H\text{-ct}}^{(q)} = 0$  in eq. (33), so that eq. (32) and eq. (33) become identical. Thus, the calculations in the MSSM and the 2HDM are the same in this case. This means that the result of class  $(q)$  derived in the MSSM for non-zero  $M_h$  is well-defined and consistent, as it corresponds to a certain special case of the general 2HDM result.

## 4.2 Inclusion of the $\tilde{t}/\tilde{b}$ sector in the on-shell scheme

For the full set of contributions to  $\Delta\rho$ , also the sfermion diagrams of class  $(\tilde{q})$  and the higgsino diagrams of class  $(\tilde{H})$  have to be taken into account. In the following, as explained above, we consider a 2HDM including also stops, sbottoms and higgsinos (although without any supersymmetric relations). The analogy of the calculation in the MSSM and the 2HDM does no longer hold, since the sfermion sector renormalization differs in the two models.

As discussed above, supersymmetry and SU(2) gauge invariance imply that not all parameters in the squark sector can be renormalized independently in the MSSM. Choosing  $m_{\tilde{b}_1}$  as the dependent mass in the MSSM, its renormalization constant  $\delta m_{\tilde{b}_1}^2$  is given by eq. (28), and no independent renormalization condition can be imposed on it. We will refer to the expression for  $\delta m_{\tilde{b}_1}^2$  in terms of the other counterterms of the fermion and sfermion sector as given in eq. (28) as the ‘‘symmetric’’ renormalization,  $\delta m_{\tilde{b}_1}^2|_{\text{symm}}$ .

In the on-shell scheme [45], the three other squark masses  $m_{\tilde{t}_{1,2}, \tilde{b}_2}$  are defined as pole masses, and the mixing angle counterterms can be defined via on-shell mixing self-energies:

$$\delta m_{\tilde{f}_i}^2 = \text{Re} \Sigma_{\tilde{f}_i}(m_{\tilde{f}_i}^2) \quad \text{for } \tilde{f}_i = \tilde{t}_{1,2}, \tilde{b}_2; \quad (38)$$

$$\delta u_{12}^{\tilde{f}} = \frac{\text{Re} \Sigma_{\tilde{f}_1 \tilde{f}_2}(m_{\tilde{f}_1}^2) + \text{Re} \Sigma_{\tilde{f}_1 \tilde{f}_2}(m_{\tilde{f}_2}^2)}{2(m_{\tilde{f}_1}^2 - m_{\tilde{f}_2}^2)} \quad \text{for } \tilde{f} = \tilde{t}, \tilde{b}. \quad (39)$$

In a 2HDM with squarks, on the other hand, an on-shell renormalization can be applied for all four squark masses. In this case  $\delta m_{\tilde{b}_1}^2$  is given by

$$\delta m_{\tilde{b}_1}^2|_{\text{OS}} = \text{Re} \Sigma_{\tilde{b}_1}(m_{\tilde{b}_1}^2), \quad (40)$$

where  $\Sigma_{\tilde{b}_1}$  is the  $\tilde{b}_1$  self-energy. Hence there is a mass shift

$$\Delta m_{\tilde{b}_1}^2 = \delta m_{\tilde{b}_1}^2|_{\text{symm}} - \delta m_{\tilde{b}_1}^2|_{\text{OS}} \quad (41)$$

at the one-loop level between the mass parameter  $m_{\tilde{b}_1}^2$  as given by the ‘‘symmetric’’ renormalization and the physical pole mass.

For the class  $(\tilde{q}, \tilde{H})$  the decomposition of  $\Delta\rho$  in the two models is given by

$$\Delta\rho_{\text{MSSM}}^{(\tilde{q}, \tilde{H})} = \Delta\rho_{2\text{-loop}}^{(\tilde{q}, \tilde{H})} + \Delta\rho_{tb\text{-ct}}^{(\tilde{q}, \tilde{H})} + \Delta\rho_{\tilde{t}\tilde{b}\text{-ct, symm}}^{(\tilde{q}, \tilde{H})} \quad (42)$$

$$\Delta\rho_{\text{2HDM}}^{(\tilde{q}, \tilde{H})} = \Delta\rho_{2\text{-loop}}^{(\tilde{q}, \tilde{H})} + \Delta\rho_{tb\text{-ct}}^{(\tilde{q}, \tilde{H})} + \Delta\rho_{\tilde{t}\tilde{b}\text{-ct, full OS}}^{(\tilde{q}, \tilde{H})} + \Delta\rho_{H\text{-ct}}^{(\tilde{q}, \tilde{H})}. \quad (43)$$

Here  $\Delta\rho_{\tilde{t}\tilde{b}\text{-ct, symm}}^{(\tilde{q}, \tilde{H})}$  corresponds to the ‘‘symmetric’’ renormalization of the squark sector in the MSSM described above.  $\Delta\rho_{\tilde{t}\tilde{b}\text{-ct, full OS}}^{(\tilde{q}, \tilde{H})}$  denotes the contribution from the full on-shell renormalization of all squarks. As one can see from eqs. (42) and (43) the MSSM result differs from the 2HDM result even for the case where  $\Delta\rho_{H\text{-ct}}^{(q)} = 0$ . The MSSM result therefore does not correspond to a special case of the 2HDM expression.

### 4.3 Result for $\Delta\rho$ in the on-shell scheme

The total result for  $\Delta\rho$  at  $\mathcal{O}(\alpha_t^2, \alpha_t\alpha_b, \alpha_b^2)$  in the MSSM is given by the sum of eqs. (32) and (42),

$$\Delta\rho^{(q, \tilde{q}, \tilde{H})} = \Delta\rho_{\text{MSSM}}^{(q)} + \Delta\rho_{\text{MSSM}}^{(\tilde{q}, \tilde{H})}. \quad (44)$$

As discussed above, in  $\Delta\rho_{\text{MSSM}}^{(\tilde{q}, \tilde{H})}$  the ‘‘symmetric’’ renormalization in the sfermion sector has to be applied, leading to the relations (15), (28) for  $m_{\tilde{b}_1}^2$  and  $\delta m_{\tilde{b}_1}^2$ . The contribution of class

$(\tilde{q}, \tilde{H})$  can be rewritten by using the mass shift as defined in eq. (41) (see also Ref. [24]), leading to the expression

$$\Delta\rho^{(q, \tilde{q}, \tilde{H})} = \Delta\rho_{\text{MSSM}}^{(q)} + \Delta\rho_{\text{MSSM, full OS}}^{(\tilde{q}, \tilde{H})} + \Delta m_{\tilde{b}_1}^2 \partial_{m_{\tilde{b}_1}^2} \Delta\rho_{1\text{-loop}}^{\text{SUSY}}, \quad (45)$$

where  $\Delta\rho_{\text{MSSM, full OS}}^{(\tilde{q}, \tilde{H})}$  is given by

$$\Delta\rho_{\text{MSSM, full OS}}^{(\tilde{q}, \tilde{H})} = \Delta\rho_{2\text{-loop}}^{(\tilde{q}, \tilde{H})} + \Delta\rho_{tb\text{-ct}}^{(\tilde{q}, \tilde{H})} + \Delta\rho_{\tilde{t}\tilde{b}\text{-ct, full OS}}^{(\tilde{q}, \tilde{H})}. \quad (46)$$

$\Delta\rho_{\text{MSSM}}^{(q)}$  is the result for the fermion-loop contributions as obtained in Ref. [27] (employing an on-shell renormalization of the fermion masses and inserting non-zero values for  $M_h$ ).  $\Delta\rho_{\text{MSSM, full OS}}^{(\tilde{q}, \tilde{H})}$  is the contribution of the squark and higgsino diagrams obtained by renormalizing *all* sfermion masses, i.e. including  $m_{\tilde{b}_1}^2$ , on-shell, while the last term in eq. (45) is a symmetry-restoring contribution involving  $\Delta m_{\tilde{b}_1}^2$ . The one-loop sfermion contribution  $\Delta\rho_{1\text{-loop}}^{\text{SUSY}}$  has been defined in eq. (5).

Comparing eqs. (46) and (43) shows that the “full OS” contribution in eq. (46) is UV-finite already for the partial gauge-less limit of eq. (36), according to the discussion of the previous two subsections.

Consistency requires that the mass shift in eq. (41) has to be UV-finite as well. One can easily check that this requires to take into account both squark/Higgs and quark/higgsino loops. Correspondingly, because of the necessity of this shift only the sum of the  $(\tilde{q})$  and  $(\tilde{H})$  contributions to  $\Delta\rho$  is physically meaningful in the MSSM.

Moreover, the mass shift  $\Delta m_{\tilde{b}_1}^2$  is only finite in the gauge-less limit, i.e. it can only consistently be evaluated if all the gauge-less limit relations (22a)–(22c) *and*  $M_h = 0$ , eq. (23), are used. The last term in eq. (45) can therefore only be obtained in the approximation where  $M_h = 0$ .

The expression in eq. (45) represents the main result of this paper. For the first term on the right-hand side of eq. (45),  $\Delta\rho_{\text{MSSM}}^{(q)}$ , we keep the full dependence on  $M_h$ . As explained above, this is possible because this term is not affected by the renormalization in the sfermion sector. For the second term,  $\Delta\rho_{\text{MSSM, full OS}}^{(\tilde{q}, \tilde{H})}$ , we will keep the  $M_h$ -dependence as well and compare to the strict gauge-less limit case where  $M_h = 0$ . The mass shift  $\Delta m_{\tilde{b}_1}^2$  entering the last term in eq. (45) is evaluated for  $M_h = 0$ .

The last term in eq. (45) can be expressed using eqs. (42) and (43) as

$$\Delta m_{\tilde{b}_1}^2 \partial_{m_{\tilde{b}_1}^2} \Delta\rho_{1\text{-loop}}^{\text{SUSY}} = \Delta\rho_{\tilde{t}\tilde{b}\text{-ct, symm}}^{(\tilde{q}, \tilde{H})} \Big|_{M_h=0} - \Delta\rho_{\tilde{t}\tilde{b}\text{-ct, full OS}}^{(\tilde{q}, \tilde{H})} \Big|_{M_h=0}. \quad (47)$$

Correspondingly the full result can be rewritten as

$$\begin{aligned} \Delta\rho^{(q, \tilde{q}, \tilde{H})} &= \Delta\rho_{\text{MSSM}}^{(q)} + \Delta\rho_{2\text{-loop}}^{(\tilde{q}, \tilde{H})} + \Delta\rho_{tb\text{-ct}}^{(\tilde{q}, \tilde{H})} + \Delta\rho_{\tilde{t}\tilde{b}\text{-ct, full OS}}^{(\tilde{q}, \tilde{H})} \\ &\quad + \left[ \Delta\rho_{\tilde{t}\tilde{b}\text{-ct, symm}}^{(\tilde{q}, \tilde{H})} \Big|_{M_h=0} - \Delta\rho_{\tilde{t}\tilde{b}\text{-ct, full OS}}^{(\tilde{q}, \tilde{H})} \Big|_{M_h=0} \right]. \end{aligned} \quad (48)$$

All contributions in the first line of eq. (48) can be evaluated by keeping the full  $M_h$  dependence. For the other parameters of the Higgs sector we impose the gauge-less limit as specified in (22a)–(22c).



As a result of eq. (37), the gauge-less limit can be relaxed in another way. If the sum of all contributions  $(q, \tilde{q}, \tilde{H})$  is considered, the relation  $\delta M_{H^\pm}^2 = \delta M_A^2$  in eq. (37) is valid. As a consequence, in the evaluation of the first line of eq. (48) it is not even necessary to use the gauge-less limit for  $\sin \alpha$  and  $M_H$ . Instead,  $\sin \alpha$  and  $M_H$  can be set to their true MSSM values. We will discuss the case where the gauge-less limit is relaxed also for these two parameters below.

## 4.4 Renormalization in the $\overline{\text{DR}}$ scheme

As an alternative to the on-shell scheme in the squark sector, we also consider the  $\overline{\text{DR}}$  scheme. In this scheme the counterterms of the soft supersymmetry-breaking parameters are defined to be pure divergences. The squark mass and mixing angle counterterms receive finite contributions corresponding to  $m_{t,b}$  in the squark mass matrices (10), (11):

$$\delta m_{\tilde{f}_i}^2|_{\text{fin}} = \left( U^{\tilde{f}} \delta \mathcal{M}_{\tilde{f}}^2 U^{\tilde{f}\dagger} \right)_{ii} \text{ for } \tilde{f}_i = \tilde{t}_{1,2}, \tilde{b}_{1,2}; \quad (49)$$

$$\delta u_{12}^{\tilde{f}}|_{\text{fin}} = \frac{\left( U^{\tilde{f}} \delta \mathcal{M}_{\tilde{f}}^2 U^{\tilde{f}\dagger} \right)_{12}}{m_{\tilde{f}_1}^2 - m_{\tilde{f}_2}^2}, \quad (50)$$

$$\delta \mathcal{M}_{\tilde{f}}^2|_{\text{fin}} = \delta m_f|_{\text{fin}} \begin{pmatrix} 2m_f & X_f \\ X_f & 2m_f \end{pmatrix}. \quad (51)$$

The result for  $\Delta\rho^{(q,\tilde{q},\tilde{H})}$  in the  $\overline{\text{DR}}$  scheme follows from eq. (48) by replacing  $\Delta\rho_{\tilde{t}\tilde{b}\text{-ct, full OS}}^{(\tilde{q},\tilde{H})}$  by the corresponding counterterm resulting from eqs. (49)–(51). As a consequence, the terms in the second line of eq. (48) vanish. The results in the  $\overline{\text{DR}}$  scheme depend on the renormalization scale  $\mu^{\overline{\text{DR}}}$ .

## 5 Numerical analysis

In this section the numerical effect of the electroweak two-loop correction eq. (45), or equivalently eq. (48), is analyzed, using the formulas in eq. (1) to obtain the corresponding shift in  $M_W$  and  $\sin^2 \theta_{\text{eff}}$ . In addition to the full MSSM correction resulting from  $\Delta\rho^{(q,\tilde{q},\tilde{H})}$ , we also present the effective change compared to the SM result (where the SM Higgs boson mass has been set to  $M_h$ ). This effective change can be decomposed into the contribution from class  $(q)$  and from classes  $(\tilde{q}, \tilde{H})$ . The contribution from class  $(q)$ , which was studied in Ref. [27], reads

$$\Delta\rho^{(q)}(\text{MSSM} - \text{SM}) = \Delta\rho_{\text{MSSM}}^{(q)} - \Delta\rho_{2\text{-loop}}^{\text{SM},\alpha_t^2}(M_{H^{\text{SM}}} = M_h), \quad (52)$$

where  $\Delta\rho_{2\text{-loop}}^{\text{SM},\alpha_t^2}$  has been given in eq. (9). The contribution from classes  $(\tilde{q}, \tilde{H})$  is given by

$$\Delta\rho^{(\tilde{q},\tilde{H})} = \Delta\rho_{\text{MSSM, full OS}}^{(\tilde{q},\tilde{H})} + \Delta m_{b_1}^2 \partial_{m_{\tilde{t}_1}^2} \Delta\rho_{1\text{-loop}}^{\text{SUSY}}, \quad (53)$$

where  $M_h = 0$  is used in the second term. Here and in the following we drop the subscript “MSSM” for simplicity.

As SM input parameters we use the values  $m_t = 178.0$  GeV,  $m_b = 3$  GeV. The bottom quark mass is to be understood as an effective bottom quark mass, taking into account higher-order QCD corrections.

## 5.1 Impact of relaxing the gauge-less limit for $M_h$ and $\sin \alpha$

In the first step we study the impact of evaluating  $\Delta\rho_{\text{MSSM, full OS}}^{(\tilde{q}, \tilde{H})}$  (see eq. (53)) for the true value of the lightest MSSM Higgs-boson mass  $M_h$  rather than for  $M_h = 0$ . Accordingly, we compare the effect on the EWPO resulting from  $\Delta\rho^{(q)}(M_h) + \Delta\rho^{(\tilde{q}, \tilde{H})}(M_h)$  and  $\Delta\rho^{(q)}(M_h) + \Delta\rho^{(\tilde{q}, \tilde{H})}(0)$ .

We have investigated the numerical effect of keeping the dependence on  $M_h$  in the squark and higgsino contributions for various MSSM scenarios. Fig. 5 shows an example where the numerical impact on the prediction of  $M_W$  and  $\sin^2 \theta_{\text{eff}}$  is quite sizable. The EWPO are given as a function of  $M_A$  with  $M_{\text{SUSY}} = -A_{t,b} = 400$  GeV,  $\mu = 800$  GeV and  $\tan \beta = 50$ . The effect of keeping a non-vanishing value of  $M_h$  in the squark and higgsino contributions amounts to about +5 MeV in  $M_W$  and  $-3 \times 10^{-5}$  to  $\sin^2 \theta_{\text{eff}}$  for all considered  $M_A$  values. The effects for other MSSM scenarios are typically smaller than for the example shown in Fig. 5. Unless otherwise stated, we will always keep the full  $M_h$  dependence in the results shown below. The difference between the result with and without the  $M_h$  dependence can be employed for estimating the residual theoretical uncertainties from unknown higher-order corrections, see the discussion in Sect. 5.4 below.

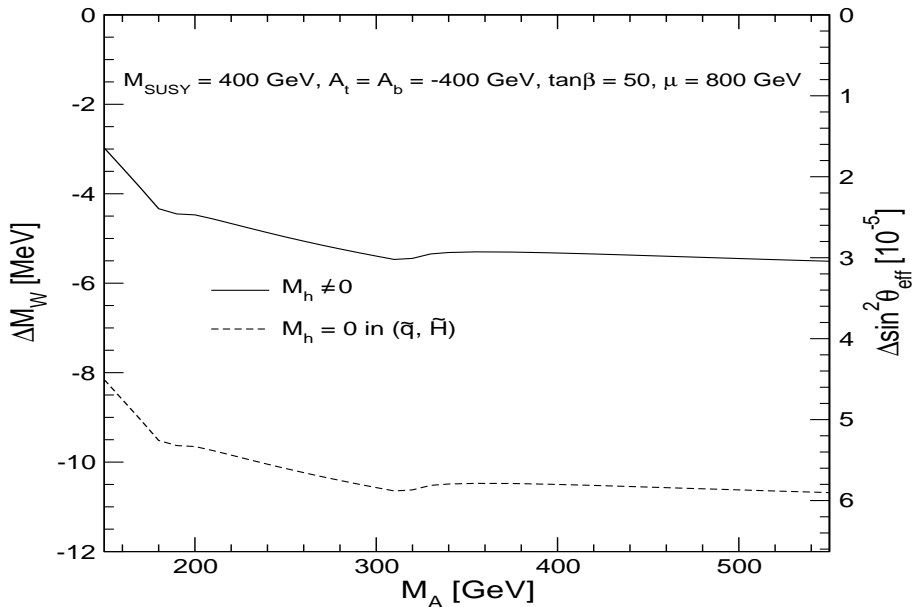


Figure 5:  $\Delta M_W$  and  $\Delta \sin^2 \theta_{\text{eff}}$  are shown as a function for  $M_A$  for the case where the full dependence on the mass of the light  $\mathcal{CP}$ -even Higgs boson is kept,  $\Delta\rho^{(q)}(M_h) + \Delta\rho^{(\tilde{q}, \tilde{H})}(M_h)$ , and for the case where the strict gauge-less limit for  $M_h$  has been applied in the squark and higgsino contributions,  $\Delta\rho^{(q)}(M_h) + \Delta\rho^{(\tilde{q}, \tilde{H})}(0)$ .

Fig. 6 illustrates the numerical effect of relaxing the gauge-less limit on  $\sin \alpha$ . As discussed at the end of Sect. 4.3, the sum of the contributions of classes  $(q, \tilde{q}, \tilde{H})$  can be evaluated in a meaningful way even if  $\sin \alpha$  and  $M_H$  are set to their true values in the MSSM instead of their values in the gauge-less limit. Since the corresponding shift in  $M_H$  is usually quite small [33] we do not analyze the effects arising from different choices for  $M_H$  and use its gauge-less value throughout the paper. The situation is different for the Higgs mixing angle  $\alpha$ . Here the

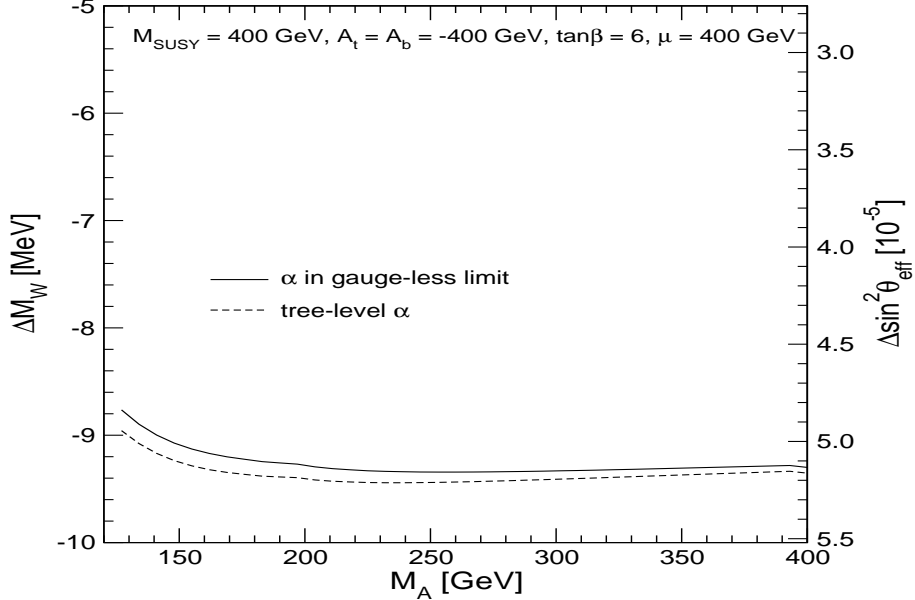


Figure 6:  $\Delta M_W$  and  $\Delta \sin^2 \theta_{\text{eff}}$  are shown for the case where the Higgs mixing angle  $\alpha$  obeys either the full tree-level relation, eq. (17), or is fixed by the gauge-less limit, eq. (22b).

full tree-level value  $\sin \alpha^{\text{full}}$  as given in eq. (17) can significantly deviate from its gauge-less value,  $\sin \alpha^{\text{gl}} = -\cos \beta$ . Fig. 6 shows the results for  $\Delta M_W$  and  $\Delta \sin^2 \theta_{\text{eff}}$  based on  $\sin \alpha^{\text{full}}$  and  $\sin \alpha^{\text{gl}}$ . The parameters are chosen in such a way as to maximize the influence of  $\sin \alpha^{\text{full}}$  vs.  $\sin \alpha^{\text{gl}}$ . The value  $\tan \beta = 6$  is rather small, and e.g. together with  $M_A = 150$  GeV it leads to  $\sin \alpha^{\text{full}} = -0.31$  and  $\sin \alpha^{\text{gl}} = -0.16$ . For  $M_{\text{SUSY}} = \mu = 400$  GeV and  $A_{t,b} = -800$  this parameter set is in agreement with all experimental constraints from Higgs boson searches [47, 48] and  $b$ -physics [49]. Fig. 6 shows that even in this scenario the numerical effect of relaxing the gauge-less limit on  $\sin \alpha$  is negligible. We have checked that this holds in general. In particular for larger  $\tan \beta$  and/or  $M_A$  the effect is even smaller. Therefore we will always set  $\sin \alpha$  to  $\sin \alpha^{\text{gl}}$  in the following.

## 5.2 Dependence on supersymmetric parameters

In Figs. 7, 8 and 10 we explore the numerical impact of  $\Delta \rho^{(q, \tilde{q}, \tilde{H})}$  on  $M_W$  and  $\sin^2 \theta_{\text{eff}}$  for various MSSM parameter choices. The values are chosen such that experimental constraints are fulfilled for most parts of the parameter space. Fig. 7 shows a scenario with large  $\tan \beta$ ,  $\tan \beta = 50$ , and  $M_{\text{SUSY}} = M_A = 300$  GeV and  $\mu = 500$  GeV. The results are plotted as functions of the stop-mixing parameter  $X_t = A_t - \mu / \tan \beta$  (see eq. (10)), and we chose  $A_b = A_t$ . The two-loop contributions  $\Delta M_W$  and  $\Delta \sin^2 \theta_{\text{eff}}$  are decomposed into the SM result,  $\Delta \rho_{2\text{-loop}}^{\text{SM}, \alpha_t^2}(M_{H^{\text{SM}}} = M_h)$ , as given in eq. (9) (shown with reversed sign for better visibility),  $\Delta \rho^{(q)}$  (MSSM – SM) as given in eq. (52), and  $\Delta \rho^{(\tilde{q}, \tilde{H})}$  as given in eq. (53). For the latter contribution both the result with the correct MSSM value for  $M_h$  and with  $M_h = 0$  is shown. We find that  $\Delta \rho^{(\tilde{q}, \tilde{H})}$  induces shifts in  $M_W$  and  $\sin^2 \theta_{\text{eff}}$  of up to +8 MeV in  $M_W$  and  $-4 \times 10^{-5}$  in  $\sin^2 \theta_{\text{eff}}$ . The corrections are significantly larger than the effective change compared to the SM arising from class (q),  $\Delta \rho^{(q)}$  (MSSM – SM). The impact of relaxing

the gauge-less limit on  $M_h$  in  $\Delta\rho^{(\tilde{q},\tilde{H})}$  is clearly visible, although not as pronounced as in Fig. 5. It should be noted that small mixing in the stop sector (in this scenario values of  $|X_t| \lesssim 350$  GeV) is disfavored by the LEP Higgs searches [47, 48], i.e. the dependence on  $M_h$  is largest where its value is already experimentally excluded. For small values of  $|X_t|$  the supersymmetric contribution  $\Delta\rho^{(q)}(\text{MSSM} - \text{SM}) + \Delta\rho^{(\tilde{q},\tilde{H})}$  is almost as large as the SM result,  $\Delta\rho_{2\text{-loop}}^{\text{SM},\alpha_t^2}(M_{H^{\text{SM}}} = M_h)$ , and largely compensates it. For large values of  $|X_t|$  the supersymmetric contribution reduces the SM result by about 40%.

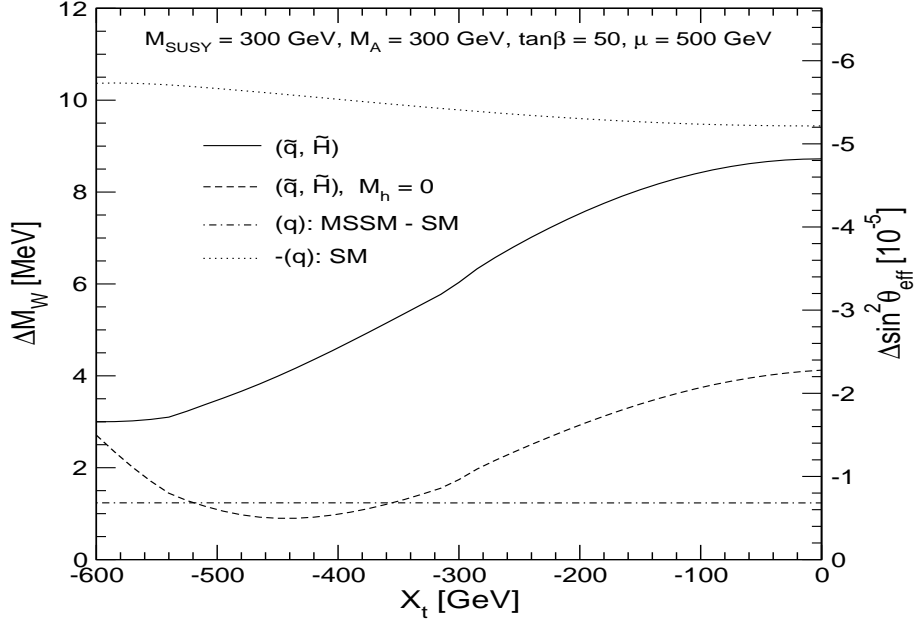


Figure 7:  $\Delta M_W$  and  $\Delta \sin^2 \theta_{\text{eff}}$  are shown as a function of  $X_t$  in a scenario with large  $\tan \beta$ . The two-loop contribution involving squarks and higgsinos,  $\Delta\rho^{(\tilde{q},\tilde{H})}$ , is shown for the correct MSSM value of  $M_h$  and for  $M_h = 0$ . For the class  $(q)$  the effective change from the SM to the MSSM is shown and compared with the pure SM contribution (with the sign reversed for better visibility).

In Fig. 8 we show a similar plot for a parameter scenario with small Higgsino mass,  $\mu = 200$  GeV, and  $\tan \beta = 6$ ,  $M_{\text{SUSY}} = 400$  GeV,  $M_A = 300$  GeV. The contribution of  $\Delta\rho^{(\tilde{q},\tilde{H})}$  amounts to about 1–2 MeV in  $M_W$  and  $-1 \times 10^{-5}$  in  $\sin^2 \theta_{\text{eff}}$  in this case. The fermion loop contribution  $\Delta\rho^{(q)}(\text{MSSM} - \text{SM})$  is very small here because the small value of  $\tan \beta$  does not lead to an enhancement of  $\alpha_b$  in the MSSM with respect to the SM.

Fig. 9 shows the one-loop results,  $\Delta\rho_{1\text{-loop}}^{\text{SUSY}}$ , corresponding to the scenarios of Figs. 7, 8. Due to the larger value of  $M_{\text{SUSY}}$  and the small value of  $\tan \beta$  the one-loop contributions for the second scenario are relatively small. The region of small  $|X_t|$  is again ruled out by LEP Higgs searches. The largest effects visible in Fig. 9 are thus experimentally excluded. Comparing the one-loop with the two-loop results, one can see that the two-loop contributions from  $\Delta\rho^{(\tilde{q},\tilde{H})}$  amounts to about 10% of the one-loop supersymmetric contributions.

A common feature of the two scenarios, visible in Figs. 7, 8, 9, is that both the one- and two-loop supersymmetric contributions first decrease for increasing  $|X_t|$  until a minimum is reached in the vicinity of  $X_t \sim -2M_{\text{SUSY}}$ . For even larger mixing one stop mass becomes very small and the supersymmetric contributions increase again.

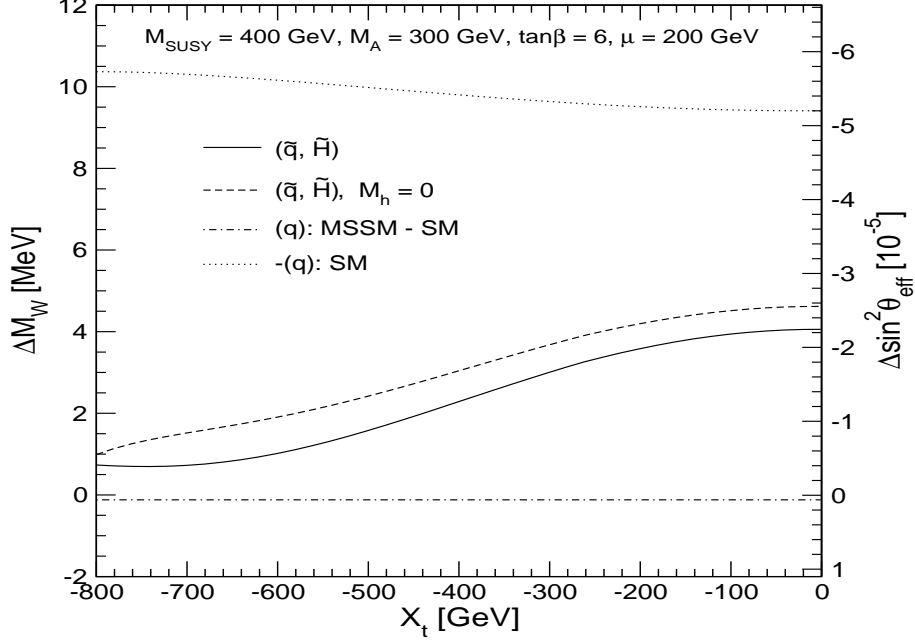


Figure 8:  $\Delta M_W$  and  $\Delta \sin^2 \theta_{\text{eff}}$  are shown as a function of  $X_t$  in a scenario with small  $\mu$  and  $\tan \beta$ . The two-loop contribution involving squarks and higgsinos,  $\Delta \rho^{(\tilde{q}, \tilde{H})}$ , is shown for the correct MSSM value of  $M_h$  and for  $M_h = 0$ . For the class  $(q)$  the effective change from the SM to the MSSM is shown and compared with the pure SM contribution (with the sign reversed for better visibility).

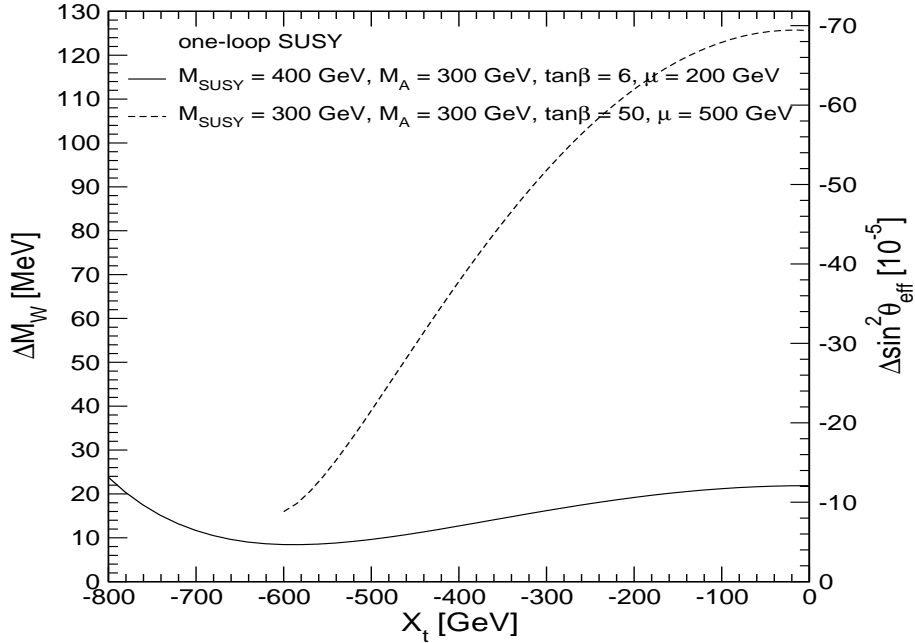


Figure 9: One-loop SUSY contributions to  $\Delta M_W$  and  $\Delta \sin^2 \theta_{\text{eff}}$  are shown as a function of  $X_t$ . The parameters correspond to the two scenarios analyzed in Figs. 7 and 8.

### 5.3 Results in SPS scenarios and renormalization scheme dependence

Fig. 10 shows the results for  $\Delta\rho^{(\tilde{q},\tilde{H})}$  in the SPS 1a benchmark scenario [29] for a moderate value of  $\tan\beta = 10$  and four different combinations for  $\mu$  and  $M_A$ ,

$$(\mu/\text{GeV}, M_A/\text{GeV}) = (200, 200), (200, 1000), (500, 500), (500, 1000). \quad (54)$$

In order to display the dependence on the scale of supersymmetry, we start from the nominal values of the MSSM parameters corresponding to the SPS 1a point [29] (besides  $\mu$  and  $M_A$  that are chosen as specified in eq. (54)) and vary the parameters  $M_{\text{SUSY}}$  and  $A_{t,b}$  using a common scale factor; the results are then shown as functions of  $M_{\text{SUSY}}$ .<sup>1</sup> The range of  $M_{\text{SUSY}}$  values shown in Fig. 10 has been chosen such that compatibility with Higgs-boson mass [48] and  $b$ -physics [49] constraints is ensured for most parts of the parameter space. For small values of  $M_{\text{SUSY}}$  the corrections differ by up to 4 MeV depending on the choice of  $M_A$  and  $\mu$ . Smaller values of  $M_A$  and  $\mu$  result in larger corrections to  $M_W$  and  $\sin^2\theta_{\text{eff}}$ . In all cases the result decreases with increasing  $M_{\text{SUSY}}$  as expected. The corresponding supersymmetric one-loop contributions induced by  $\Delta\rho_{1\text{-loop}}^{\text{SUSY}}$  are shown in Fig. 11 for comparison. The two-loop correction from  $\Delta\rho^{(\tilde{q},\tilde{H})}$  amounts up to 25% of the MSSM one-loop result.

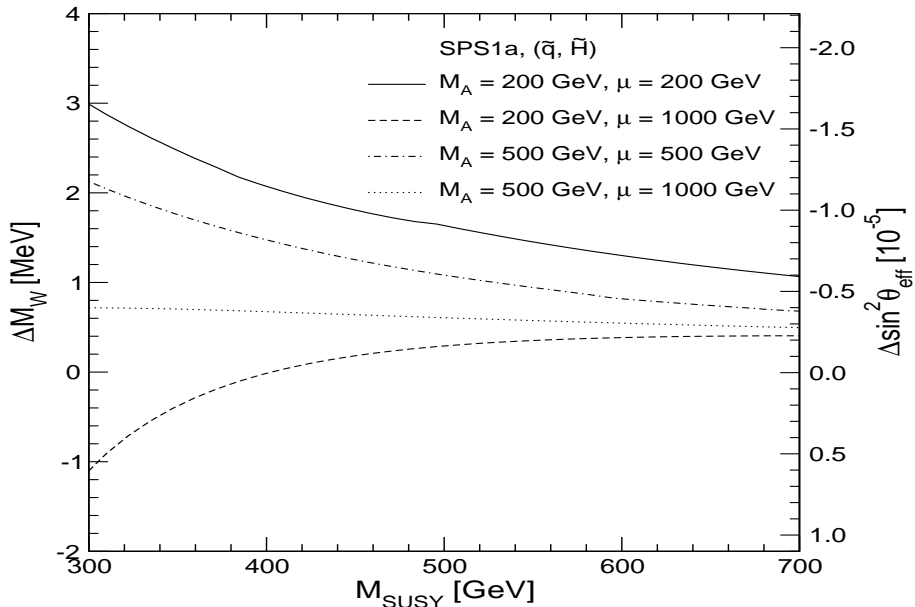


Figure 10: The shifts  $\Delta M_W$  and  $\Delta\sin^2\theta_{\text{eff}}$  induced by  $\Delta\rho^{(\tilde{q},\tilde{H})}$  are shown as a function of  $M_{\text{SUSY}}$  in the SPS 1a scenario for four combinations of  $M_A = 200, 500$  GeV and  $\mu = 200, 500, 1000$  GeV.

We now study the renormalization scheme dependence of the one-loop and two-loop results for three benchmark SPS scenarios. Besides the “standard” scenario SPS 1a, we also investigate the SPS 1b scenario, which is characterized by a larger  $\tan\beta$  value,  $\tan\beta = 30$ ,

<sup>1</sup>More precisely, for the SPS points the soft supersymmetry-breaking parameters  $M_{\tilde{t}_L, \tilde{t}_R, \tilde{b}_R}$  for the left- and right-handed  $\tilde{t}$ ,  $\tilde{b}$  are all slightly different.  $M_{\text{SUSY}}$  is identified with  $M_{\tilde{t}_L}$ .

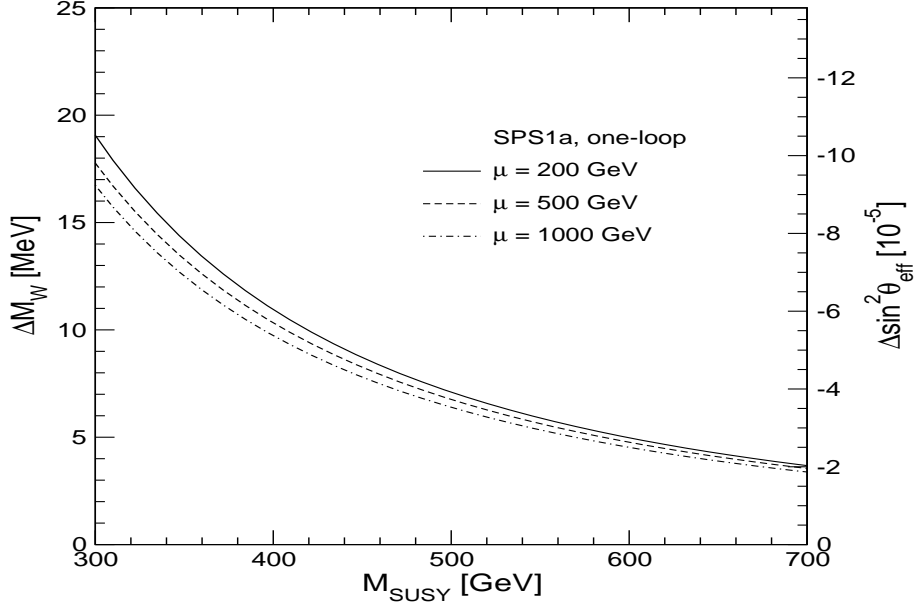


Figure 11: The shifts  $\Delta M_W$  and  $\Delta \sin^2 \theta_{\text{eff}}$  induced by the supersymmetric one-loop contributions are shown as a function of  $M_{\text{SUSY}}$  in the SPS 1a scenario for  $\mu = 200, 500, 1000$  GeV and  $\tan \beta = 10$ .

and SPS 5, which involves a relatively light  $\tilde{t}$  [29]. Fig. 12 shows the one-loop results for the three scenarios, while Figs. 13, 14, 15 display the two-loop results. As above, the results are shown as functions of  $M_{\text{SUSY}}$ . We have started from the nominal values of the MSSM parameters for the three benchmark points and varied the parameters  $M_{\text{SUSY}}, A_{t,b}, \mu$  (for the  $\overline{\text{DR}}$  results also the scale  $\mu^{\overline{\text{DR}}}$ ) using a common scale factor. The actual SPS 1a, SPS 1b and SPS 5 benchmark points correspond to  $M_{\text{SUSY}} = 495.9, 762.5, 535.2$  GeV, respectively [29].

For a meaningful comparison of the results in the on-shell and the  $\overline{\text{DR}}$  renormalization schemes, the input parameters in the two schemes have to be physically equivalent, which implies that they are numerically different. Since the parameters in the SPS scenarios are defined as  $\overline{\text{DR}}$  parameters, they can directly be used as input parameters in the  $\overline{\text{DR}}$  scheme. The corresponding input parameters for the calculation in the on-shell scheme are obtained by requiring

$$(m_{\tilde{f}_i}^2 + \delta m_{\tilde{f}_i}^2)^{\text{OS}} = (m_{\tilde{f}_i}^2 + \delta m_{\tilde{f}_i}^2)^{\overline{\text{DR}}} \quad (55)$$

for the squark masses and similarly for the mixing angles.

In the one-loop results  $\Delta \rho_{1\text{-loop}}^{\text{SUSY}}$  for the three SPS scenarios shown in Fig. 12 the squark sector parameters correspond to the on-shell scheme. The shift in the precision observables induced by  $\Delta \rho_{1\text{-loop}}^{\text{SUSY}}$  is found to be particularly large for the SPS 5 scenario, as a consequence of the large splitting between the squark masses in this scenario.

In Figs. 13–15 we show the one-loop result parametrized in terms of on-shell parameters (dotted line) and the two-loop ( $\tilde{q}, \tilde{H}$ ) results obtained in the  $\overline{\text{DR}}$  (full line) and the OS scheme (dot-dashed line), in all cases relative to the one-loop result parametrized in terms of the

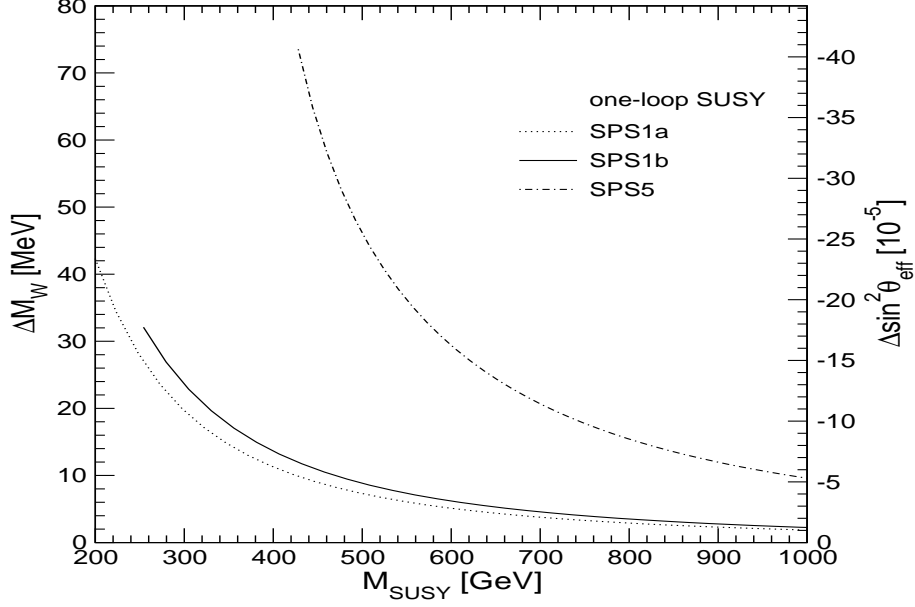


Figure 12: The shifts  $\Delta M_W$  and  $\Delta \sin^2 \theta_{\text{eff}}$  induced by the supersymmetric one-loop contribution  $\Delta \rho_{1\text{-loop}}^{\text{SUSY}}$  are shown for the three benchmark scenarios SPS 1a, SPS 1b and SPS 5 as a function of  $M_{\text{SUSY}}$ . The parameters of the squark sector correspond to the on-shell scheme.

$\overline{\text{DR}}$  parameters. Accordingly, the three lines in each plot correspond to

$$\left\{ \begin{array}{l} \Delta \rho_{1\text{-loop}}^{\text{SUSY,OS}} \\ \Delta \rho_{1\text{-loop}}^{\text{SUSY},\overline{\text{DR}}} + \Delta \rho^{(\tilde{q},\tilde{H}),\overline{\text{DR}}} \\ \Delta \rho_{1\text{-loop}}^{\text{SUSY,OS}} + \Delta \rho^{(\tilde{q},\tilde{H}),\text{OS}} \end{array} \right\} - \Delta \rho_{1\text{-loop}}^{\text{SUSY},\overline{\text{DR}}}. \quad (56)$$

The pure two-loop correction in the  $\overline{\text{DR}}$  scheme is given by the full line, while the two-loop correction in the on-shell scheme corresponds to the difference between the dot-dashed and the dashed line.

The numerical impact of the two-loop correction  $\Delta \rho^{(\tilde{q},\tilde{H})}$  in the scenarios SPS 1a, 1b amounts to about 5–6 MeV in  $M_W$  and  $-3 \times 10^{-5}$  in  $\sin^2 \theta_{\text{eff}}$  for small  $M_{\text{SUSY}}$  and decreases to about 1 MeV in  $M_W$  ( $-0.5 \times 10^{-5}$  in  $\sin^2 \theta_{\text{eff}}$ ) for larger values of  $M_{\text{SUSY}}$ . For SPS 5 the corrections are slightly smaller. While in the scenarios SPS 1a, 1b the two-loop results in the two schemes are very close to each other, a larger deviation is visible in the SPS 5 scenario. In the latter scenario the two-loop corrections in the on-shell scheme are less than 1 MeV, while in the  $\overline{\text{DR}}$  scheme they are more than twice as large. Comparison with the one-loop results given in Fig. 12 shows that the two-loop corrections amount to about 10% one-loop MSSM contribution.

The comparison of the renormalization schemes shows that the scheme dependence is strongly reduced by going from the one-loop to the two-loop level. At the one-loop level, where the scheme difference is entirely due to the different input parameters for the squark masses and mixing angles, the difference between the on-shell and the  $\overline{\text{DR}}$  scheme is of  $\mathcal{O}(1 \text{ MeV})$  in  $M_W$ . Taking into account the two-loop corrections reduces the difference below 0.1 MeV for SPS 1a,b and about 0.2 MeV for SPS 5.



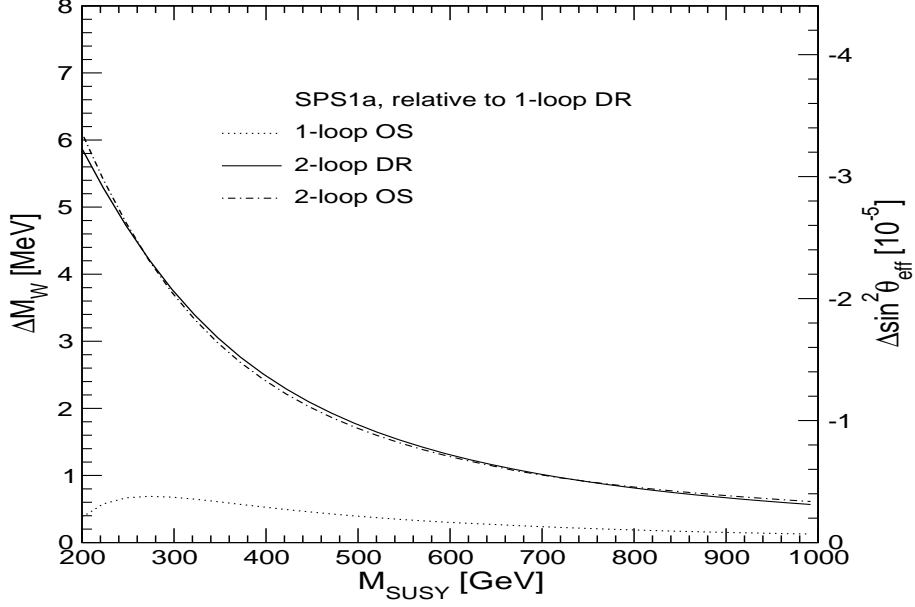


Figure 13:  $\Delta M_W$  and  $\Delta \sin^2 \theta_{\text{eff}}$  are shown in the SPS 1a scenario as a function of  $M_{\text{SUSY}}$ . The results for the one-loop contribution expressed in terms of on-shell parameters and for the two-loop result  $\Delta \rho_{1\text{-loop}}^{\text{SUSY}} + \Delta \rho^{(\tilde{q}, \tilde{H})}$  in the on-shell and the  $\overline{\text{DR}}$  scheme are given relative to the one-loop result expressed in terms of  $\overline{\text{DR}}$  parameters, see eq. (56).

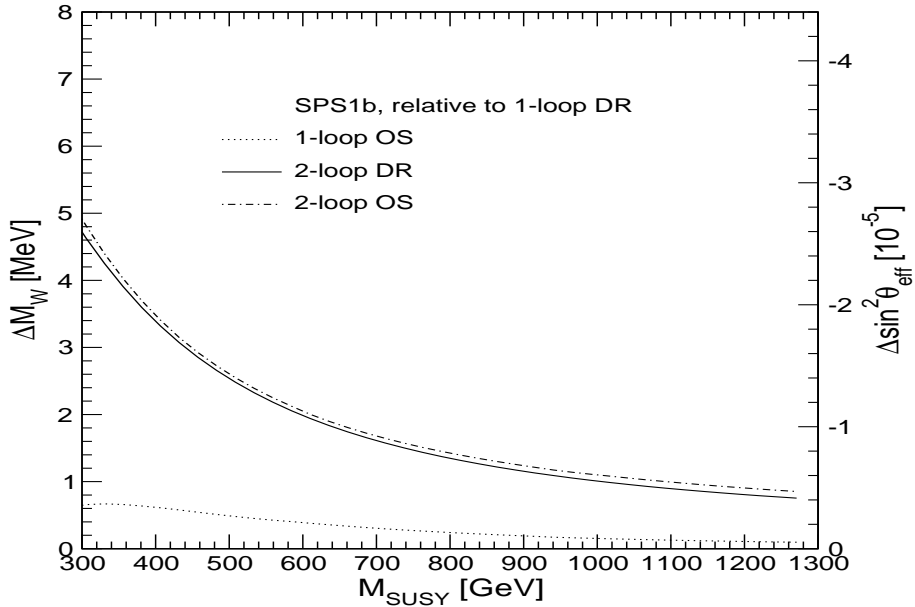


Figure 14:  $\Delta M_W$  and  $\Delta \sin^2 \theta_{\text{eff}}$  are shown in the SPS 1b scenario as a function of  $M_{\text{SUSY}}$ . The results for the one-loop contribution expressed in terms of on-shell parameters and for the two-loop result  $\Delta \rho_{1\text{-loop}}^{\text{SUSY}} + \Delta \rho^{(\tilde{q}, \tilde{H})}$  in the on-shell and the  $\overline{\text{DR}}$  scheme are given relative to the one-loop result expressed in terms of  $\overline{\text{DR}}$  parameters, see eq. (56).

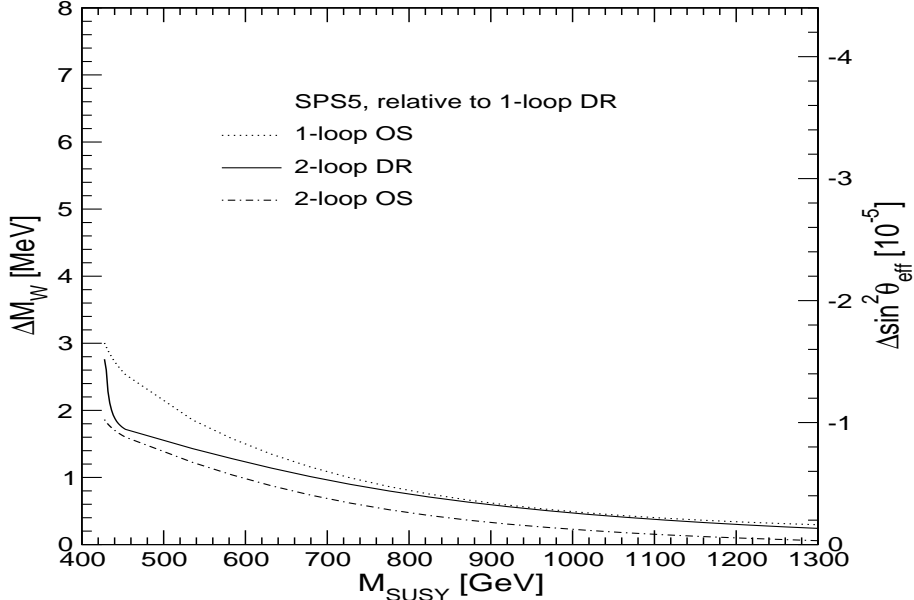


Figure 15:  $\Delta M_W$  and  $\Delta \sin^2 \theta_{\text{eff}}$  are shown in the SPS 5 scenario as a function of  $M_{\text{SUSY}}$ . The results for the one-loop contribution expressed in terms of on-shell parameters and for the two-loop result  $\Delta\rho_{1\text{-loop}}^{\text{SUSY}} + \Delta\rho^{(\tilde{q}, \tilde{H})}$  in the on-shell and the  $\overline{\text{DR}}$  scheme are given relative to the one-loop result expressed in terms of  $\overline{\text{DR}}$  parameters, see eq. (56).

The size of the two-loop corrections for SPS 1a,b is found to be much larger than the difference between the two schemes at the one-loop level, which is only about 1 MeV for these scenarios. This indicates that the difference between the results in two renormalization schemes, if taken as the only measure for estimating the theoretical uncertainties from unknown higher-order corrections, may result in a significant underestimate of the actual theoretical uncertainty. The SPS 5 scenario, on the other hand, is an example where the two-loop corrections turn out to be smaller than the scheme difference at one-loop order.

Finally we compare the two-loop results for the  $(\tilde{q}, \tilde{H})$  contributions obtained in this paper with the two-loop QCD corrections of  $\mathcal{O}(\alpha_s)$  as obtained in Ref. [24]. In Fig. 16 we show the results in the on-shell scheme for the three SPS scenarios as a function of  $M_{\text{SUSY}}$  (as explained above). For SPS 1a and 1b both corrections are roughly of the same size and compensate each other to a large extent. Only for the case of SPS 5 the QCD corrections are significantly larger than the two-loop Yukawa corrections. Both the QCD and the Yukawa corrections are non-negligible in view of the anticipated future experimental accuracies and larger than the current theoretical uncertainties in the SM.

## 5.4 Estimate of unknown higher-order corrections

As discussed above, the theoretical evaluation of the EWPO in the SM is significantly more advanced than in the MSSM. In order to obtain an accurate prediction for the EWPO within the MSSM it is therefore useful to take all known SM corrections into account. This can be

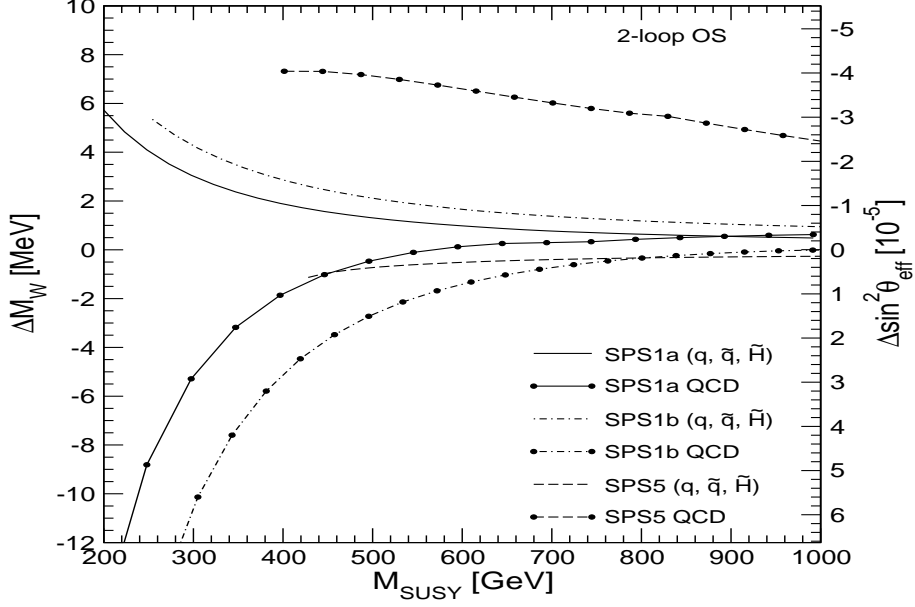


Figure 16: The effect of the two-loop Yukawa corrections from squark and higgsino loops is compared with the squark-loop corrections of  $\mathcal{O}(\alpha_s)$ .  $\Delta M_W$  and  $\Delta \sin^2 \theta_{\text{eff}}$  are shown in the three SPS scenarios as a function of  $M_{\text{SUSY}}$  in the on-shell scheme.

done by writing the MSSM prediction for the observable  $O$  ( $O = M_W, \sin^2 \theta_{\text{eff}}, \dots$ ) as

$$O_{\text{MSSM}} = O_{\text{SM}} + O_{\text{MSSM-SM}} , \quad (57)$$

where  $O_{\text{SM}}$  is the prediction in the SM including all known corrections, and  $O_{\text{MSSM-SM}}$  is the difference between the MSSM and the SM predictions, evaluated at the level of precision of the known MSSM corrections. The expression given in eq. (57) contains higher-order contributions that are only known for SM particles in the loop but not for their superpartners (e.g. two-loop electroweak corrections beyond the leading Yukawa contributions calculated in this paper and three-loop corrections of  $\mathcal{O}(\alpha_s^2)$ ). In the decoupling limit where all superpartners are heavy and the Higgs sector becomes SM-like, the result of eq. (57) obviously yields a more precise prediction than a result based on only those corrections which are known in the full MSSM. In this case the second term in eq. (57) goes to zero, so that the MSSM result approaches the SM result with  $M_{H^{\text{SM}}} = M_h$ . For lower values of the scale of supersymmetry the contribution from supersymmetric particles in the the loop may be of comparable size as the known SM corrections. In view of the experimental bounds on the masses of the supersymmetric particles (and the fact that supersymmetry has to be broken), however, a complete cancellation between the SM and supersymmetric contributions is not expected. It therefore seems appropriate to apply eq. (57) also in this case.

Expressing the predictions for the EWPO as in eq. (57) implies that the theoretical uncertainties from unknown higher-order corrections reduce to those in the SM in the decoupling limit. In the SM, based on all higher-order contributions that are currently known, the remaining uncertainties in  $M_W$  [8] and  $\sin^2 \theta_{\text{eff}}$  [9] have been estimated to be

$$\delta M_W^{\text{SM}} = 4 \text{ MeV}, \quad \delta \sin^2 \theta_{\text{eff}}^{\text{SM}} = 5 \times 10^{-5} . \quad (58)$$

Below the decoupling limit an additional theoretical uncertainty arises from higher-order corrections involving supersymmetric particles in the loops. In the following we will estimate this additional theoretical uncertainty in the prediction of  $M_W$  and  $\sin^2 \theta_{\text{eff}}$  depending on the supersymmetric parameters. We will provide estimates for the uncertainty for three values of the squark mass scale,  $M_{\text{SUSY}} = 200, 500, 1000$  GeV. A similar approach of estimating the remaining uncertainties from unknown higher-order corrections with dependence on the supersymmetric parameters has recently been applied to the Higgs sector and implemented in the program *FeynHiggs2.2*, see Ref. [36] for details.

The remaining uncertainties from unknown higher-order corrections involving supersymmetric particles mainly arise from the following sources:

- Electroweak two-loop corrections beyond the leading Yukawa corrections evaluated in this paper:

We estimate the numerical effect of these corrections by assuming that the ratio of the subleading electroweak two-loop corrections to the two-loop Yukawa corrections is the same in the SM as in the MSSM. Inserting the known SM corrections [7, 8] we infer an estimate of the possible size of the missing supersymmetric electroweak two-loop contributions.

- $\mathcal{O}(\alpha\alpha_s)$  corrections beyond the  $\Delta\rho$  approximation:

We estimate the size of these corrections by assuming that the ratio of the contribution entering via  $\Delta\rho$  to the full result is the same as for the known SM result [50].

- $\mathcal{O}(\alpha\alpha_s^2)$  corrections:

We use three different methods for estimating the possible size of these corrections. The unknown ratio of the  $\mathcal{O}(\alpha\alpha_s^2)$  supersymmetric contributions to the  $\mathcal{O}(\alpha\alpha_s)$  supersymmetric contributions can be estimated by assuming that it is the same as for the corresponding corrections in the SM [13] (estimate (a)) and, using geometric progression from lower orders, by assuming that it is the same as the ratio of the  $\mathcal{O}(\alpha\alpha_s)$  supersymmetric contributions and the  $\mathcal{O}(\alpha)$  supersymmetric contributions (estimate (b)). As a further indication of the possible size of unknown corrections of  $\mathcal{O}(\alpha\alpha_s^2)$  we vary the renormalization scale of  $\alpha_s(\mu^{\overline{\text{DR}}})$  entering the  $\mathcal{O}(\alpha\alpha_s)$  result according to  $m_t/2 \leq \mu^{\overline{\text{DR}}} \leq 2m_t$  (estimate (c)). It should be noted that this variation of  $\alpha_s(\mu^{\overline{\text{DR}}})$  corresponds to only a part of the higher-order corrections, so that estimates (a) and (b) should be regarded as more conservative.

- $\mathcal{O}(\alpha^2\alpha_s)$  corrections:

Similarly as for the  $\mathcal{O}(\alpha\alpha_s^2)$  corrections, we again use three different methods for estimating these corrections. The unknown ratio of the  $\mathcal{O}(\alpha^2\alpha_s)$  supersymmetric contributions to the  $\mathcal{O}(\alpha^2)$  (leading Yukawa) supersymmetric contributions can be estimated by assuming that it is the same as for the corresponding corrections in the SM [18] (estimate (a)) and by assuming that it is the same as the ratio of the  $\mathcal{O}(\alpha\alpha_s)$  supersymmetric contributions and the  $\mathcal{O}(\alpha)$  supersymmetric contributions (estimate (b)). As a further indication of possible corrections of  $\mathcal{O}(\alpha^2\alpha_s)$  we change the value of  $m_t$  in the result for the two-loop supersymmetric Yukawa corrections from the on-shell value,  $m_t^{\text{OS}}$ , to the running mass  $m_t(m_t)$ , where  $m_t(m_t) = m_t^{\text{OS}}/(1 + 4/(3\pi)\alpha_s(m_t))$  (estimate (c)). The latter replacement accounts only for a subset of the unknown  $\mathcal{O}(\alpha^2\alpha_s)$  corrections.

- Electroweak three-loop corrections:

As an indication of the possible size of these corrections we use the renormalization scheme dependence of our result for the supersymmetric two-loop Yukawa corrections, see Figs. 13–15.

We have evaluated the above estimates for the three scenarios SPS 1a, SPS 1b, and SPS 5, each for  $M_{\text{SUSY}} = 1000$  GeV, 500 GeV, and for  $M_{\text{SUSY}} < 500$  GeV <sup>2</sup> (as above we have varied  $M_{\text{SUSY}}$ ,  $A_{t,b}$  and  $\mu$  using a common scale factor). The estimated theoretical uncertainties for  $M_W$  arising from the different classes of unknown higher-order corrections are shown in Tab. 1. The result given in each entry corresponds to the largest value obtained in the three considered SPS scenarios. The three numbers given for the  $\mathcal{O}(\alpha\alpha_s^2)$  and  $\mathcal{O}(\alpha^2\alpha_s)$  corrections correspond to the estimates (a), (b) and (c) described above.

$M_{\text{SUSY}}$	<500 GeV	500 GeV	1000 GeV
$\mathcal{O}(\alpha^2)$ subleading	6.0	2.0	0.8
$\mathcal{O}(\alpha\alpha_s)$ subleading	1.8	0.9	0.5
$\mathcal{O}(\alpha\alpha_s^2)$	3.0, 5.3, 1.5	1.4, 1.1, 0.7	0.9, 2.2, 0.5
$\mathcal{O}(\alpha^2\alpha_s)$	1.5, 2.2, 1.4	0.6, 0.8, 0.4	0.2, 0.2, 0.2
$\mathcal{O}(\alpha^3)$	0.3	0.3	0.3

Table 1: Estimated uncertainties for  $M_W$  in MeV for different classes of unknown higher-order corrections involving supersymmetric particles are given for three values of  $M_{\text{SUSY}}$ . The estimates have been obtained using the results for the SPS 1a, SPS 1b, and SPS 5 scenarios. The three entries for the  $\mathcal{O}(\alpha\alpha_s^2)$  and  $\mathcal{O}(\alpha^2\alpha_s)$  corrections correspond to three different methods for estimating the uncertainties (see text).

As expected, the estimated uncertainties associated with the supersymmetric higher-order contributions decrease for increasing  $M_{\text{SUSY}}$ . For the  $\mathcal{O}(\alpha\alpha_s^2)$  and  $\mathcal{O}(\alpha^2\alpha_s)$  corrections, method (c) that accounts only for a part of the higher-order corrections yields in both cases the most optimistic estimate. As discussed earlier, by taking into account the true MSSM-value of  $M_h$ , certain parts of the electroweak corrections, beyond the leading two-loop Yukawa corrections, are included in our result. The difference between  $\Delta\rho^{(\tilde{q},\tilde{H})}(M_h)$  and  $\Delta\rho^{(\tilde{q},\tilde{H})}(0)$  may be interpreted as an estimate of the size of further, not included higher-order electroweak corrections. The numerical analysis in Sects. 5.1 and 5.2 shows that this estimate is typically smaller than the estimated total uncertainty in Tab. 1.

We now combine the values given in Tab. 1 into our total estimate of the remaining theoretical uncertainties from unknown higher-order corrections involving supersymmetric particles. Adopting the largest of the three values for the  $\mathcal{O}(\alpha\alpha_s^2)$  and  $\mathcal{O}(\alpha^2\alpha_s)$  as a conser-

<sup>2</sup>The lowest values considered for  $M_{\text{SUSY}}$  are 200, 300, 400 GeV for SPS1a, SPS1b, SPS5, respectively. These are the lowest values shown in Figs. 13, 14, 15. For lower values the parameter points are excluded by Higgs mass constraints.

vative error estimate and adding the different estimates in quadrature we obtain

$$\begin{aligned}
\delta M_W &= 8.5 \text{ MeV for } M_{\text{SUSY}} < 500 \text{ GeV}, \\
\delta M_W &= 2.7 \text{ MeV for } M_{\text{SUSY}} = 500 \text{ GeV}, \\
\delta M_W &= 2.4 \text{ MeV for } M_{\text{SUSY}} = 1000 \text{ GeV}.
\end{aligned}
\tag{59}$$

An analogous analysis of the remaining higher-order uncertainties can also be carried out for  $\sin^2 \theta_{\text{eff}}$ . Since parts of the missing higher-order corrections to  $\sin^2 \theta_{\text{eff}}$  and  $M_W$  are related to each other, we employ eq. (1) to infer estimates for  $\sin^2 \theta_{\text{eff}}$  from our results for  $M_W$ . This yields

$$\begin{aligned}
\delta \sin^2 \theta_{\text{eff}} &= 4.7 \times 10^{-5} \text{ for } M_{\text{SUSY}} < 500 \text{ GeV}, \\
\delta \sin^2 \theta_{\text{eff}} &= 1.5 \times 10^{-5} \text{ for } M_{\text{SUSY}} = 500 \text{ GeV}, \\
\delta \sin^2 \theta_{\text{eff}} &= 1.3 \times 10^{-5} \text{ for } M_{\text{SUSY}} = 1000 \text{ GeV}.
\end{aligned}
\tag{60}$$

The full theory uncertainty in the MSSM can be obtained by adding in quadrature the SM uncertainties from eq. (58) and the SUSY uncertainties from eqs. (59)–(60). This yields  $\delta M_W = (4.7 - 9.4) \text{ MeV}$  and  $\delta \sin^2 \theta_{\text{eff}} = (5.2 - 6.7) \times 10^{-5}$  depending on the SUSY mass scale.

The estimated uncertainties are smaller than the estimates in Ref. [2] (where an overall estimate has been given without analyzing the dependence on the supersymmetric parameters), reflecting the improvement associated with the new corrections calculated in this paper.

The other source of theoretical uncertainties besides the one from unknown higher-order corrections is the parametric uncertainty induced by the experimental errors of the input parameters. The current experimental error of the top-quark mass [51] induces the following parametric uncertainties in  $M_W$  and  $\sin^2 \theta_{\text{eff}}$

$$\delta m_t^{\text{exp}} = 2.9 \text{ GeV} \Rightarrow \delta M_W^{\text{para}, m_t} = 17.5 \text{ MeV}, \quad \delta \sin^2 \theta_{\text{eff}}^{\text{para}, m_t} = 9.4 \times 10^{-5}. \tag{61}$$

This uncertainty will decrease during the next years as a consequence of a further improvement of the accuracy on  $m_t$  at the Tevatron and the LHC. Ultimately it will be reduced by more than an order of magnitude at the ILC [52]. The accuracy of the theoretical predictions for  $M_W$  and  $\sin^2 \theta_{\text{eff}}$  will then be limited by the uncertainty from unknown higher-order corrections (for a discussion of the parametric uncertainties induced by the other SM input parameters see Ref. [2]). A further reduction of the uncertainties from higher-order SM-type corrections (see eq. (58)) and corrections involving supersymmetric particles (see eqs. (59)–(60)) therefore seems to be in order to fully exploit the prospective experimental accuracies on  $M_W$ ,  $\sin^2 \theta_{\text{eff}}$  and  $m_t$  reachable at the next generation of colliders [52, 53].

## 6 Conclusions

In this paper we have calculated the two-loop corrections of  $\mathcal{O}(\alpha_t^2)$ ,  $\mathcal{O}(\alpha_t \alpha_b)$ ,  $\mathcal{O}(\alpha_b^2)$  to the electroweak precision observables  $M_W$  and  $\sin^2 \theta_{\text{eff}}$  in the MSSM. These are the leading, Yukawa-enhanced electroweak two-loop contributions; they enter via  $\Delta\rho$  and arise from diagrams involving SM quarks, squarks, Higgs bosons and higgsinos. While previously only the

contribution from the diagrams with quarks and Higgs bosons had been known (corresponding to the limiting case where all supersymmetric particles are infinitely heavy), we have evaluated the complete set of Yukawa corrections including the effects of supersymmetric particles.

We have given a detailed account of the theoretical basis of the calculation, focusing on the implications of the parameter relations enforced by supersymmetry. In the gauge-less limit that needs to be employed to extract the Yukawa corrections of  $\mathcal{O}(\alpha_t^2)$ ,  $\mathcal{O}(\alpha_t\alpha_b)$ ,  $\mathcal{O}(\alpha_b^2)$  the lightest MSSM Higgs boson mass  $M_h$  vanishes. We have studied in how far the true MSSM value for  $M_h$  can be taken into account in a consistent way. We have shown that the result can be expressed in such a way that the  $M_h$ -dependence, being formally a sub-leading effect, can be kept essentially everywhere and we have compared this result with the case where the gauge-less limit is strictly imposed.

In our numerical analysis we have put the main emphasis on the new supersymmetric contributions involving squarks and higgsinos. We have analyzed the results of the new contributions as functions of the squark mass scale  $M_{\text{SUSY}}$ , the stop mixing  $X_t$  and the higgsino and Higgs boson mass parameters  $\mu$  and  $M_A$ . For squark masses of about 300 GeV we find corrections of typically +4 MeV in  $M_W$  and  $-2 \times 10^{-5}$  in  $\sin^2\theta_{\text{eff}}$ . In certain parameter regions, in particular slightly smaller values of  $M_{\text{SUSY}}$  or small mixing in the stop sector, we find shifts up to +8 MeV in  $M_W$  and  $-4 \times 10^{-5}$  in  $\sin^2\theta_{\text{eff}}$ . For a wide range of parameters, the squark and higgsino two-loop corrections increase the corresponding one-loop contributions by about 10%.

Therefore, the class of diagrams with squarks and higgsinos, which has no SM counterpart, gives rise to significant deviations from the SM predictions. This is in contrast with the contribution of the diagrams involving quarks and Higgs bosons, which can be well approximated by the corresponding SM contribution (setting the SM Higgs-boson mass equal to the mass of the lightest  $\mathcal{CP}$ -even Higgs boson of the MSSM). We have compared our result for the two-loop Yukawa correction of  $\mathcal{O}(\alpha_t^2)$ ,  $\mathcal{O}(\alpha_t\alpha_b)$ ,  $\mathcal{O}(\alpha_b^2)$  to  $M_W$  and  $\sin^2\theta_{\text{eff}}$  with the  $\mathcal{O}(\alpha\alpha_s)$  correction, which is the only other genuine two-loop contribution to  $M_W$  and  $\sin^2\theta_{\text{eff}}$  known in the full MSSM. We find that the two corrections are of comparable size and can largely compensate each other for small values of  $M_{\text{SUSY}}$  (depending on the other supersymmetric parameters).

We have derived our result in two renormalization schemes, the on-shell scheme and the  $\overline{\text{DR}}$  scheme for the squark sector parameters. Comparing the two-loop results with the one-loop result expressed in terms of the parameters of the two schemes shows a significant reduction of the scheme dependence.

We have shown how the known corrections to the electroweak precision observables in the SM and the MSSM can be combined such that the currently most accurate prediction in the MSSM is obtained. In the decoupling limit, where all supersymmetric particles are heavy, the theoretical uncertainty from unknown higher-order corrections reduces to the uncertainty of the SM contribution. For non-vanishing contributions of the supersymmetric particles an additional theoretical uncertainty arises from unknown higher-order corrections involving supersymmetric particles.

We have estimated the current uncertainty from unknown higher-order corrections involving supersymmetric particles for different values of the squark mass scale  $M_{\text{SUSY}}$ . This has been done using geometric progression from lower orders, employing known results for corre-

sponding SM corrections, investigating the renormalization scheme dependence, varying the renormalization scale, and taking into account formally subleading  $M_h$ -dependent contributions. For a squark mass scale below 500 GeV we obtain an estimated uncertainty of about 8.5 MeV in  $M_W$  and  $4.5 \times 10^{-5}$  in  $\sin^2 \theta_{\text{eff}}$ . These uncertainties reduce to about 2.5 MeV in  $M_W$  and  $1.5 \times 10^{-5}$  in  $\sin^2 \theta_{\text{eff}}$  for  $M_{\text{SUSY}} = 1$  TeV. They can be combined quadratically with the theory uncertainty from unknown higher-order SM contributions to obtain the full MSSM theory uncertainties. While currently these uncertainties (for  $M_{\text{SUSY}} < 500$  GeV) are about a factor of two smaller than the parametric theoretical uncertainties induced by the experimental error of the top-quark mass, their impact will become more pronounced with the expected improvement of the experimental precision of  $m_t$ . The new two-loop corrections evaluated in this paper have been important to reduce the theoretical uncertainties to the present level. Further efforts on higher-order corrections in the MSSM will be necessary in order to reduce the theoretical uncertainties from unknown higher order corrections within the MSSM to the level that has been reached for the SM.

## Acknowledgements

We thank W. Hollik and A. Weber for helpful discussions. S.H. and G.W. thank the Max Planck Institut für Physik, München, for kind hospitality during part of this work.



## References

- [1] M. Grünewald, hep-ex/0304023; updated as:  
C. Diaconu, talk given at "Lepton-Photon 2005", Uppsala, Sweden, June 2005, see:  
[lp2005.tsl.uu.se/lp2005/LP2005/programme/presentationer/morning/diaconu.pdf](http://lp2005.tsl.uu.se/lp2005/LP2005/programme/presentationer/morning/diaconu.pdf); see also: [lepewwg.web.cern.ch/LEPEWWG/Welcome.html](http://lepewwg.web.cern.ch/LEPEWWG/Welcome.html).
- [2] S. Heinemeyer, W. Hollik and G. Weiglein, hep-ph/0412214.
- [3] J. Ellis, S. Heinemeyer, K. Olive and G. Weiglein, *JHEP* **0502** 013, hep-ph/0411216.
- [4] G. Wilson, LC-PHSM-2001-009, see: [www.desy.de/~lcnotes/notes.html](http://www.desy.de/~lcnotes/notes.html) .
- [5] U. Baur, R. Clare, J. Erler, S. Heinemeyer, D. Wackerroth, G. Weiglein and D. Wood, hep-ph/0111314.
- [6] R. Hawkings and K. Mönig, *Eur. Phys. J. direct* **C 8** (1999) 1; hep-ex/9910022.
- [7] A. Freitas, W. Hollik, W. Walter and G. Weiglein, *Phys. Lett.* **B 495** (2000) 338 [Erratum-ibid. **B 570** (2003) 260], hep-ph/0007091;  
A. Freitas, W. Hollik, W. Walter and G. Weiglein, *Nucl. Phys.* **B 632** (2002) 189 [Erratum-ibid. **B 666** (2003) 305], hep-ph/0202131;  
M. Awramik and M. Czakon, *Phys. Lett.* **B 568** (2003) 48, hep-ph/0305248;  
M. Awramik and M. Czakon, *Phys. Rev. Lett.* **89** (2002) 241801, hep-ph/0208113;  
A. Onishchenko and O. Veretin, *Phys. Lett.* **B 551** (2003) 111, hep-ph/0209010;  
M. Awramik, M. Czakon, A. Onishchenko and O. Veretin, *Phys. Rev.* **D 68** (2003) 053004, hep-ph/0209084.
- [8] M. Awramik, M. Czakon, A. Freitas and G. Weiglein, *Phys. Rev.* **D 69** (2004) 053006, hep-ph/0311148.
- [9] M. Awramik, M. Czakon, A. Freitas and G. Weiglein, *Phys. Rev. Lett.* **93** (2004) 201805, hep-ph/0407317.
- [10] W. Hollik, U. Meier and S. Uccirati, hep-ph/0507158.
- [11] M. Veltman, *Nucl. Phys.* **B 123** (1977) 89.
- [12] A. Djouadi and C. Verzegnassi, *Phys. Lett.* **B 195** (1987) 265;  
A. Djouadi, *Nuovo Cim.* **A 100** (1988) 357.
- [13] L. Avdeev et al., *Phys. Lett.* **B 336** (1994) 560 [Erratum-ibid. **B 349** (1995) 597], hep-ph/9406363;  
K. Chetyrkin, J. Kühn and M. Steinhauser, *Phys. Lett.* **B 351** (1995) 331, hep-ph/9502291; *Phys. Rev. Lett.* **75** (1995) 3394, hep-ph/9504413.
- [14] J. van der Bij and F. Hoogeveen, *Nucl. Phys.* **B 283** (1987) 477.
- [15] R. Barbieri, M. Beccaria, P. Ciafaloni, G. Curci and A. Vicere, *Nucl. Phys.* **B 409** (1993) 105;  
J. Fleischer, F. Jegerlehner and O.V. Tarasov, *Phys. Lett.* **B 319** (1993) 249.

- [16] J. van der Bij and M. Veltman, *Nucl. Phys.* **B 231** (1984) 205.
- [17] J. van der Bij, K. Chetyrkin, M. Faisst, G. Jikia and T. Seidensticker, *Phys. Lett.* **B 498** (2001) 156, hep-ph/0011373.
- [18] M. Faisst, J. Kühn, T. Seidensticker and O. Veretin, *Nucl. Phys.* **B 665** (2003) 649, hep-ph/0302275.
- [19] R. Boughezal, J. Tausk and J. van der Bij, *Nucl. Phys.* **B 713** (2005) 278, hep-ph/0410216.
- [20] H. Nilles, *Phys. Rep.* **110** (1984) 1;  
H. Haber and G. Kane, *Phys. Rep.* **117**, (1985) 75;  
R. Barbieri, *Riv. Nuovo Cim.* **11**, (1988) 1.
- [21] R. Barbieri and L. Maiani, *Nucl. Phys.* **B 224** (1983) 32;  
C. Lim, T. Inami and N. Sakai, *Phys. Rev.* **D 29** (1984) 1488;  
E. Eliasson, *Phys. Lett.* **B 147** (1984) 65;  
Z. Hioki, *Prog. Theo. Phys.* **73** (1985) 1283;  
J. Grifols and J. Solà, *Nucl. Phys.* **B 253** (1985) 47;  
B. Lynn, M. Peskin and R. Stuart, CERN Report 86-02, p. 90;  
R. Barbieri, M. Frigeni, F. Giuliani and H. Haber, *Nucl. Phys.* **B 341** (1990) 309;  
M. Drees and K. Hagiwara, *Phys. Rev.* **D 42** (1990) 1709.
- [22] M. Drees, K. Hagiwara and A. Yamada, *Phys. Rev.* **D 45** (1992) 1725;  
P. Chankowski, A. Dabelstein, W. Hollik, W. Mösle, S. Pokorski and J. Rosiek, *Nucl. Phys.* **B 417** (1994) 101;  
D. Garcia and J. Solà, *Mod. Phys. Lett.* **A 9** (1994) 211.
- [23] S. Heinemeyer, W. Hollik, F. Merz, S. Peñaranda, *Eur. Phys. J.* **C 37** (2004) 481, hep-ph/0403228.
- [24] A. Djouadi, P. Gambino, S. Heinemeyer, W. Hollik, C. Jünger and G. Weiglein, *Phys. Rev. Lett.* **78** (1997) 3626, hep-ph/9612363; *Phys. Rev.* **D 57** (1998) 4179, hep-ph/9710438.
- [25] S. Heinemeyer, PhD Thesis, Univ. Karlsruhe, Shaker Verlag, Aachen 1998, ISBN 3826537874, see [www-itp.physik.uni-karlsruhe.de/prep/phd/](http://www-itp.physik.uni-karlsruhe.de/prep/phd/);  
G. Weiglein, hep-ph/9901317.
- [26] J. Haestier, S. Heinemeyer, D. Stöckinger and G. Weiglein, *Proceedings of the 2005 International Linear Collider Workshop - Stanford, USA*, arXiv:hep-ph/0506259.
- [27] S. Heinemeyer and G. Weiglein, *JHEP* **0210** (2002) 072, hep-ph/0209305; hep-ph/0301062.
- [28] S. Heinemeyer, D. Stöckinger and G. Weiglein, *Nucl. Phys.* **B 690** (2004) 62, hep-ph/0312264; *Nucl. Phys.* **B 699** (2004) 103, hep-ph/0405255.
- [29] B. Allanach et al., *Eur. Phys. J.* **C 25** (2002) 113, hep-ph/0202233;  
The definition of the MSSM parameter for the SPS points can be found at [www.ippp.dur.ac.uk/~georg/sps/](http://www.ippp.dur.ac.uk/~georg/sps/).

- [30] A. Denner, S. Dittmaier and G. Weiglein, hep-ph/9505271.
- [31] J. Gunion, H. Haber, G. Kane and S. Dawson, *The Higgs Hunter's Guide*, Addison-Wesley, 1990.
- [32] S. Heinemeyer, hep-ph/0407244;  
A. Djouadi, hep-ph/0503173.
- [33] S. Heinemeyer, W. Hollik and G. Weiglein, *Comp. Phys. Comm.* **124** 2000 76, hep-ph/9812320; *Eur. Phys. J. C* **9** (1999) 343, hep-ph/9812472. The code is accessible via [www.feynhiggs.de](http://www.feynhiggs.de) .
- [34] M. Frank, S. Heinemeyer, W. Hollik and G. Weiglein, hep-ph/0202166.
- [35] G. Degrassi, S. Heinemeyer, W. Hollik, P. Slavich and G. Weiglein, *Eur. Phys. J. C* **28** (2003) 133, hep-ph/0212020.
- [36] T. Hahn, S. Heinemeyer, W. Hollik and G. Weiglein, hep-ph/0507009;  
M. Frank, T. Hahn, S. Heinemeyer, W. Hollik and G. Weiglein, *in preparation*.
- [37] J. Küblbeck, M. Böhm and A. Denner, *Comp. Phys. Comm.* **60** (1990) 165;  
T. Hahn and M. Perez-Victoria, *Comput. Phys. Comm.* **118** (1999) 153, hep-ph/9807565;  
T. Hahn, *Nucl. Phys. Proc. Suppl.* **89** (2000) 231, hep-ph/0005029; *Comput. Phys. Comm.* **140** (2001) 418, hep-ph/0012260.  
The program is available via [www.feynarts.de](http://www.feynarts.de) .
- [38] T. Hahn and C. Schappacher, *Comput. Phys. Comm.* **143** (2002) 54, hep-ph/0105349.
- [39] G. Weiglein, R. Scharf and M. Böhm, *Nucl. Phys. B* **416** (1994) 606, hep-ph/9310358;  
G. Weiglein, R. Mertig, R. Scharf and M. Böhm, in *New Computing Techniques in Physics Research 2*, ed. D. Perret-Gallix (World Scientific, Singapore, 1992), p. 617.
- [40] D. Stöckinger, *TYReduce*, unpublished.
- [41] G. Passarino and M. Veltman, *Nucl. Phys. B* **160** (1979) 151.
- [42] A. Davydychev und J. Tausk, *Nucl. Phys. B* **397** (1993) 123;  
F. Berends und J. Tausk, *Nucl. Phys. B* **421** (1994) 456.
- [43] G. 't Hooft and M. Veltman, *Nucl. Phys. B* **44** (1972) 189;  
C. Bollini and J. Giambiagi, *Nuovo Cimento B* **12** (1972) 20;  
J. Ashmore, *Nuovo Cimento Lett.* **4** (1972) 289.
- [44] W. Siegel, *Phys. Lett. B* **84** (1979) 193;  
D. Capper, D. Jones and P. van Nieuwenhuizen, *Nucl. Phys. B* **167** (1980) 479;  
W. Siegel, *Phys. Lett. B* **94** (1980) 37;  
L. Avdeev, *Phys. Lett. B* **117** (1982) 317;  
L. Avdeev and A. Vladimirov, *Nucl. Phys. B* **219** (1983) 262;  
I. Jack and D. Jones, hep-ph/9707278, in *Perspectives on Supersymmetry*, ed. G. Kane (World Scientific, Singapore), p. 149;  
D. Stöckinger, *JHEP* **0503** (2005) 076, hep-ph/0503129.

- [45] W. Hollik, E. Kraus, M. Roth, C. Rupp, K. Sibold and D. Stöckinger, *Nucl. Phys. B* **639** (2002) 3, hep-ph/0204350;  
W. Hollik and H. Rzehak, *Eur. Phys. J. C* **32** (2003) 127, hep-ph/0305328.
- [46] S. Heinemeyer, W. Hollik, H. Rzehak and G. Weiglein, *Eur. Phys. J. C* **39** (2005) 465  
hep-ph/0411114.
- [47] G. Abbiendi et al. [ALEPH, DELPHI, L3, OPAL Collaborations and LEP Working Group for Higgs boson searches], hep-ex/0107030, hep-ex/0107031.
- [48] G. Abbiendi et al. [ALEPH, DELPHI, L3, OPAL Collaborations and LEP Working Group for Higgs boson searches], *Phys. Lett. B* **565** (2003) 61, hep-ex/0306033.
- [49] S. Eidelman et al. [Particle Data Group Collaboration], *Phys. Lett. B* **592** (2004) 1.
- [50] B. Kniehl, *Nucl. Phys. B* **347** (1990) 89;  
F. Halzen and B. Kniehl, *Nucl. Phys. B* **353** (1991) 567;  
B. Kniehl and A. Sirlin, *Nucl. Phys. B* **371** (1992) 141; *Phys. Rev. D* **47** (1993) 883;  
A. Djouadi and P. Gambino, *Phys. Rev. D* **49** (1994) 3499 [Erratum-ibid. **D 53** (1994) 4111], hep-ph/9309298.
- [51] J.F. Arguin et al. [The CDF Collaboration, the D0 Collaboration and the Tevatron Electroweak Working Group], hep-ex/0507091.
- [52] S. Heinemeyer, S. Kraml, W. Porod and G. Weiglein, *JHEP* **0309** (2003) 075, hep-ph/0306181.
- [53] S. Heinemeyer, T. Mannel and G. Weiglein, hep-ph/9909538;  
J. Erler, S. Heinemeyer, W. Hollik, G. Weiglein and P. Zerwas, *Phys. Lett. B* **486** (2000) 125, hep-ph/0005024;  
J. Erler and S. Heinemeyer, hep-ph/0102083.